








# Climate change promotes transitions to tall evergreen vegetation in tropical Asia

Simon Scheiter<sup>1</sup>  | Dushyant Kumar<sup>1</sup>  | Richard T. Corlett<sup>2,3</sup>  |  
 Camille Gaillard<sup>1</sup>  | Liam Langan<sup>1</sup>  | Ralph Sedricke Lapuz<sup>2,4</sup>  | Carola Martens<sup>1,5</sup>  |  
 Mirjam Pfeiffer<sup>1</sup>  | Kyle W. Tomlinson<sup>2,3</sup> 

<sup>1</sup>Senckenberg Biodiversity and Climate Research Centre (SBiK-F), Frankfurt am Main, Germany

<sup>2</sup>Center for Integrative Conservation, Xishuangbanna Tropical Botanical Garden, Chinese Academy of Sciences, Menglun, Yunnan, China

<sup>3</sup>Center of Conservation Biology, Core Botanical Gardens, Chinese Academy of Sciences, Menglun, Yunnan, China

<sup>4</sup>University of Chinese Academy of Sciences, Beijing, China

<sup>5</sup>Institute of Physical Geography, Goethe-University Frankfurt am Main, Frankfurt am Main, Germany

## Correspondence

Simon Scheiter, Senckenberg Biodiversity and Climate Research Centre (SBiK-F), Senckenberganlage 25, 60325 Frankfurt am Main, Germany.  
 Email: [simon.scheiter@senckenberg.de](mailto:simon.scheiter@senckenberg.de)

## Funding information

Deutsche Forschungsgemeinschaft, Grant/Award Number: SCHE 1719/2-1; Natural Science Foundation of China – Yunnan Government, Grant/Award Number: U1502264; German Federal Ministry of Education and Research, Grant/Award Number: 01LL1802B and 01LL1801B; CAS-TWAS President's Fellowship for International Doctoral Students, Grant/Award Number: 2016CTF096

## Abstract

Vegetation in tropical Asia is highly diverse due to large environmental gradients and heterogeneity of landscapes. This biodiversity is threatened by intense land use and climate change. However, despite the rich biodiversity and the dense human population, tropical Asia is often underrepresented in global biodiversity assessments. Understanding how climate change influences the remaining areas of natural vegetation is therefore highly important for conservation planning. Here, we used the adaptive Dynamic Global Vegetation Model version 2 (aDGVM2) to simulate impacts of climate change and elevated CO<sub>2</sub> on vegetation formations in tropical Asia for an ensemble of climate change scenarios. We used climate forcing from five different climate models for representative concentration pathways RCP4.5 and RCP8.5. We found that vegetation in tropical Asia will remain a carbon sink until 2099, and that vegetation biomass increases of up to 28% by 2099 are associated with transitions from small to tall woody vegetation and from deciduous to evergreen vegetation. Patterns of phenology were less responsive to climate change and elevated CO<sub>2</sub> than biomes and biomass, indicating that the selection of variables and methods used to detect vegetation changes is crucial. Model simulations revealed substantial variation within the ensemble, both in biomass increases and in distributions of different biome types. Our results have important implications for management policy, because they suggest that large ensembles of climate models and scenarios are required to assess a wide range of potential future trajectories of vegetation change and to develop robust management plans. Furthermore, our results highlight open ecosystems with low tree cover as most threatened by climate change, indicating potential conflicts of interest between biodiversity conservation in open ecosystems and active afforestation to enhance carbon sequestration.

## KEYWORDS

aDGVM2, biome shifts, climate change, CO<sub>2</sub> fertilization, model ensemble, phenology, tropical Asia

This is an open access article under the terms of the Creative Commons Attribution License, which permits use, distribution and reproduction in any medium, provided the original work is properly cited.

© 2020 The Authors. *Global Change Biology* published by John Wiley & Sons Ltd

## 1 | INTRODUCTION

Tropical Asia includes seven of the 36 global biodiversity hotspots identified by Zachos and Habel (2011). These hotspots are characterized by high diversity and endemism, and they are threatened due to habitat loss (Hughes, 2017). Habitat and biodiversity loss in tropical Asia can be attributed to a variety of direct and indirect anthropogenic impacts. Direct impacts include land-cover change, for example by deforestation, conversion to cropland, plantations or other agricultural land use, and associated fragmentation (Hughes, 2017). Indirect impacts include regional and global climate change caused by anthropogenic emissions of greenhouse gases such as carbon dioxide (CO<sub>2</sub>), methane (CH<sub>4</sub>) and nitrous oxide (N<sub>2</sub>O). These changes in the composition of the atmosphere and changes in radiative forcing are the drivers of climate change (IPCC, 2018). Atmospheric CO<sub>2</sub> concentrations also directly influence plant growth and productivity (Chen et al., 2019; Piao et al., 2020) and, along with climate change, broad-scale distribution patterns of species, biomes and biodiversity.

Indirect impacts will likely have the largest effects in remaining areas with intact vegetation that are protected from direct human impacts, such as legally protected areas. Yet, direct human impacts have already caused substantial losses of biodiversity in tropical Asia (Hughes, 2017). Many protected areas are under pressure by increasing human population and land use intensities in neighbouring buffer zones, or by changes in their protection status (Symes, Rao, Mascia, & Carrasco, 2016). Hannah et al. (2020) showed that species extinction risk in the tropics could be halved if 30% of the land surface were protected and climate change limited to 2°C. Understanding indirect anthropogenic effects on undisturbed vegetation is therefore crucial to implement effective measures in conservation, land management and climate change mitigation.

Two important features of vegetation that can respond to climate change at local scale, and thereby influence large-scale patterns of vegetation distribution, carbon storage and biodiversity, are vegetation structure and plant phenology. Features of vegetation structure, such as woody cover, stem density, growth form and vegetation height, determine habitat suitability for animals (Smit & Prins, 2015; Tews et al., 2004) and link different trophic levels via biotic interaction networks (Schleuning et al., 2016; Walther, 2010). Vegetation structure and canopy characteristics also influence the near-surface microclimatic conditions, as well as albedo, surface roughness and partitioning of energy into sensible and latent heat fluxes (Bonan, 2008; Ozanne et al., 2003). These properties of the land surface couple biosphere, atmosphere and hydrosphere, and influence climate–vegetation feedbacks (Bonan, 2008; Zeng et al., 2017).

Plant phenology describes periodic life cycle events that are ultimately caused by seasonal and interannual variations in climate. It determines events such as leaf green-up, flowering and leaf senescence, and whether a plant is evergreen or a deciduous. Changes in phenology as a result of climate change have already been observed (Buitenwerf, Rose, & Higgins, 2015; Cleland, Chuine, Menzel, Mooney, & Schwartz, 2007) and may have implications for

biodiversity (Piao et al., 2019; Walther, 2010). Phenology influences biosphere–atmosphere coupling through seasonal and intraannual variations in albedo and biogeochemical fluxes (Bonan, 2008; Piao et al., 2019).

Understanding the impacts of climate change on vegetation structure and phenology is essential to assess potential future vegetation dynamics, ecosystem functioning and to develop policy recommendations. Such an assessment requires (a) the capacity to predict plant growth and vegetation dynamics in response to climate conditions, atmospheric CO<sub>2</sub> concentration, soil conditions and disturbance regimes; (b) estimates of the uncertainties associated with different climate change scenarios; and (c) a set of variables or vegetation classification schemes relevant for policy to track and quantify vegetation change.

Dynamic global vegetation models (DGVMs, Prentice et al., 2007) are widely used tools for simulation of vegetation dynamics and biogeochemical cycles. These models use eco-physiological principles to simulate vegetation dynamics at large spatio-temporal scales. DGVMs can include mechanistic representations of disturbances such as fire (Hantson et al., 2016; Scheiter & Higgins, 2009) or herbivory (Pachzelt, Rammig, Higgins, & Hickler, 2013; Pfeiffer et al., 2019), and biotic interactions such as competition for space, water, nutrients and light (Prentice et al., 2007). DGVMs simulate transient vegetation dynamics in response to fluctuating climate conditions and are often used as land surface schemes in general circulation models (GCMs, e.g. JSBACH, Reick, Raddatz, Brovkin, & Gayler, 2013). Conducting DGVM simulations for ensembles of climate change scenarios derived from different GCMs allows estimating potential future trajectories and to assess uncertainties. Variables and classification schemes for quantifying vegetation states and change can be tailored to specific research questions or specific study areas, or to procedures used for model testing. For example, basal area and vegetation height derived from field measurements can be used to quantify vegetation structure, eddy covariance measurements to quantify biogeochemical cycles, or biome distributions from remote sensing or modelling to quantify vegetation shifts. The selection of an appropriate set of variables is crucial, because it can influence whether a change is detected or not.

Despite the size and rich biodiversity of tropical Asia, this region remains underrepresented in global biodiversity assessments (Hughes, 2017) and in DGVM studies. While the region is included in global-scale DGVM simulations (e.g. Hickler, Prentice, Smith, Sykes, & Zaehle, 2006; Sato, Itoh, & Kohyama, 2007; Smith et al., 2014), studies explicitly focusing on this region are rare (Chaturvedi et al., 2011; Kumar & Scheiter, 2019; Ravindranath, Joshi, Sukumar, & Saxena, 2006). Accordingly, important features of vegetation at regional scale might not be well represented in global-scale simulations. One feature in this regard is the Asian savanna. These ecosystems are often misinterpreted as degraded forest, with afforestation being considered as appropriate conservation policy (Kumar, Pfeiffer, Gaillard, Langan, Martens, et al., 2020; Ratnam, Tomlinson, Rasquinha, & Sankaran, 2016). Models often simulate savanna areas as forest (Kumar & Scheiter, 2019).

A second feature not well represented in models is the distribution of deciduous and evergreen vegetation in mainland Southeast Asia. Due to rainfall seasonality, deciduous vegetation stretches from Myanmar to Vietnam, bordered by semi-evergreen and evergreen forests. This pattern is, for example, not represented in global simulations conducted with lund-potsdam-jena general ecosystem simulator (LPJ-GUESS) (Smith et al., 2014) or SEIB-DGVM (Sato et al., 2007), but is simulated by an LPJ-GUESS version that includes a complex representation of hydrology (Hickler et al., 2006) and by a JSBACH version with variable traits (Verheijen et al., 2013). Representing this vegetation feature correctly is particularly important as changes in rainfall seasonality and an increasing frequency of droughts are predicted for tropical Asia (Hijioka et al., 2014; Zhang et al., 2016).

Here, we used a dynamic vegetation model, the adaptive Dynamic Global Vegetation Model version 2 (aDGVM2, Langan, Higgins, & Scheiter, 2017; Scheiter, Langan, & Higgins, 2013), to simulate current and future vegetation states in tropical Asia for an ensemble of the Coupled Model Intercomparison Project 5 (CMIP5) climate change projections provided by the Inter-Sectoral Impact Model Intercomparison Project (ISIMIP; Warszawski et al., 2014). To assess possible trajectories of future vegetation and quantify related uncertainties, we conducted simulations for an ensemble of two different representative concentration pathways (RCP4.5 and RCP8.5) and five different GCMs. We used different variables and classification schemes to track vegetation states and vegetation change under future climate conditions. We expected (a) that elevated CO<sub>2</sub> will lead to higher woody biomass until 2099 due to CO<sub>2</sub> fertilization, even in areas where precipitation decreases; (b) that these biomass changes will be associated with vegetation changes from shorter and deciduous vegetation towards taller and evergreen vegetation; (c) that variation within the simulated future vegetation states will be substantial due to variation within the ensemble of climate model projections, as well as stochastic effects in aDGVM2; and (d) that the area affected by vegetation change will be influenced by the variables used to track vegetation changes. In addition, we assessed how consideration of managed and cultivated land (Tuanmu & Jetz, 2014) modifies the area affected by climate change.

## 2 | MATERIALS AND METHODS

### 2.1 | aDGVM2 model description

We used aDGVM2, an individual-based dynamic vegetation model that is based on concepts from community assembly theory and uses a functional trait approach. The aDGVM2 concept and a detailed model description are provided by Kumar, Pfeiffer, Gaillard, Langan, and Scheiter (2020), Langan et al. (2017), and Scheiter et al. (2013). A short summary of the model description is provided in the Supporting Information. Model variables used in the analyses are described in the following paragraphs.

### 2.2 | Environmental forcing data

We simulated vegetation for tropical Asia (South Asia, Southeast Asia, tropical China) for an ensemble of historic and future climate change trajectories. We used climate forcing compiled for the ISIMIP (Warszawski et al., 2014). These data comprise daily time series of bias-corrected and statistically downscaled climate variables at 0.5° spatial resolution between 1950 and 2099. We used minimum, maximum and average near-surface air temperature, precipitation, near-surface relative humidity, near-surface wind speed and downwelling long- and short-wave radiation. We used climate data for RCP4.5 and RCP8.5 for five different GCMs: GFDL-ESM2M, HadGEM2-ES, IPSL-CM5A-LR, MIROC-ESM-CHEM and NorESM1-M (Warszawski et al., 2014). Time series of mean annual precipitation and temperature for each ensemble member averaged for the entire study region are provided in Figure S1.

We used RCP8.5 because it represents the worst-case scenario within all RCPs, with high carbon emissions, high energy consumption and low climate mitigation until 2099 (van Vuuren et al., 2011). In RCP4.5, it was assumed that carbon emissions peak towards the middle of the century and decrease afterwards. Cropland and utilized grassland areas decreased in RCP4.5 to the benefit of other vegetation types (van Vuuren et al., 2011), and feedbacks between such vegetation changes and the climate were considered. These two scenarios cover a range of possible scenarios and envelope the intermediate scenario RCP6.0. We decided to omit RCP2.6, a low-emission scenario with ambiguous climate mitigation and negative emissions, for example, by carbon capture and storage techniques.

Soil data were derived from the Harmonized World Soil Database (Nachtergaele, van Velthuizen, & Verelst, 2009) and we used elevation from the Shuttle Radar Topography Mission (Jarvis, Reuter, Nelson, & Guevara, 2008). Atmospheric CO<sub>2</sub> concentrations were derived from van Vuuren et al. (2011) for RCP4.5 and RCP8.5. Model simulations were conducted at 1° spatial resolution (see Section 2.3). Therefore, climate, soil and elevation data were re-sampled to the required 1° spatial resolution using the nearest neighbour method.

### 2.3 | Model simulations

We conducted aDGVM2 ensemble simulations for tropical Asia at 1° spatial resolution and daily temporal resolution using climate data of five GCMs for RCP4.5 and RCP8.5 (Section 2.2), amounting to 10 scenarios in total. Replicate runs for these scenarios were not conducted due to the high computational demands. For each simulation, we conducted a 450-year model spin-up to allow modelled state variables, traits and plant communities to reach a dynamic equilibrium with environmental conditions. For model spin-up, we used a random sequence of years from the period between 1950 and 1980 for each ensemble member. After the spin-up, transient simulations were conducted using the time series between 1950 and 2099 of the respective scenario. Simulations were conducted in the presence of a natural surface fire regime, as represented

by the aDGVM2 fire routines (Langan et al., 2017; Supporting Information). Anthropogenic fire was not simulated. We simulated potential natural vegetation in the absence of anthropogenic impacts (but see Section 2.8). All data processing procedures and model analyses were conducted with R (R Core Team, 2018) and the 'raster' package (Hijmans, 2020).

## 2.4 | Biome types

The aDGVM2 simulates biomass, phenology and height of individual woody plants (trees or shrubs) and grass patches, as well as plant population characteristics at plot level, such as number of plants or height structure. We used model state variables to classify vegetation in a grid cell into different biome types. To account for vegetation structure and phenology, we tailored a classification scheme that reflects these features. The classification scheme distinguishes seven different biomes characterized by evergreen and deciduous, tall and short woody vegetation, and woody and grassy vegetation.

When simulated woody cover in a grid cell is below 10% and aboveground grass biomass (including both  $C_3$  and  $C_4$  grasses) is below 300 kg/ha, vegetation is classified as desert. When woody cover is below 10% and aboveground grass biomass (including both  $C_3$  and  $C_4$  grasses) is above 300 kg/ha, vegetation is classified as  $C_3$  or  $C_4$  grassland, depending on the fractional cover of the grass types. If woody cover exceeds 10%, vegetation is classified as woody vegetation, irrespective of grass biomass. Woody vegetation is subdivided into the four combinations of evergreen and deciduous as well as short and tall. Vegetation is classified as evergreen if the number of evergreen woody plants exceeds the number of deciduous woody plants; otherwise, it is classified as deciduous. Woody vegetation is classified as short if the 90th percentile of the plant height distribution is less than 4 m, otherwise it is classified as tall. The 4-m threshold was picked because application of different thresholds showed that the simulated distribution of tall vegetation derived from the 4-m threshold agreed well with observed forest distribution (Haxeltine & Prentice, 1996). In studies using both observations and models, vegetation height is typically not used in biome classification (for an exception using remote sensing data see Higgins, Buitenwerf, & Moncrieff, 2016).

In our biome scheme we assume that the four woody vegetation types include shrubland, savanna, woodland and different forest types. These types of woody vegetation are functionally different and often used in vegetation mapping, both using models and using observations from field studies or remote sensing. However, here we used four woody vegetation types to be able to focus on features related to phenology and vegetation height, and to constrain the number of biome types. In Kumar, Pfeiffer, Gaillard, Langan, Martens, et al. (2020) and Kumar, Pfeiffer, Gaillard, Langan, and Scheiter (2020), we included different types of woody vegetation, and highlighted the importance of distinguishing between savanna and dry deciduous forest.

Biome classification was conducted for each grid cell and each ensemble member to obtain biome maps for each ensemble member.

Consensus biome maps for each RCP were then generated by identifying the most frequent biome type in the ensemble in each grid cell. We tracked the number of ensemble members that represent the consensus biome type in each RCP as a proxy for model uncertainty.

## 2.5 | Dominant phenological type

The aDGVM2 simulates four different phenological strategies: light-triggered evergreen, rain-triggered evergreen, light-triggered deciduous and rain-triggered deciduous (for details see Supporting Information and Langan et al., 2017). To investigate the patterns of phenological strategies and their responses to climate change, we calculated the relative abundance of woody plants of each phenological strategy in each simulated grid cell. We assigned a dominant phenological type to each grid cell based on the most abundant phenological strategy of woody plants. We tracked both changes in the relative abundances of different phenological strategies and of the dominant phenological strategy in response to climate change.

Phenology classification was conducted for each grid cell and each ensemble member to obtain maps of the dominant phenology type for each ensemble member. Consensus maps of the dominant phenological type for each RCP were generated by identifying the most frequent dominant phenological type in the ensemble in each simulated grid cell. We tracked the number of ensemble members that represent the consensus-dominant phenological type in each RCP as a proxy for model uncertainty.

## 2.6 | Benchmarking

Kumar, Pfeiffer, Gaillard, Langan, and Scheiter (2020) parameterized aDGVM2 for South Asia (i.e. the western areas of the study region) and conducted data-model comparisons using multiple remote sensing products. Here, we compared simulated vegetation of all ensemble members and the ensemble means for both RCPs for current climate conditions (year 2019) to biomass and height derived from remote sensing. For biomass, we used the product of Saatchi et al. (2011), and for vegetation height we used the product of Simard, Pinto, Fisher, and Baccini (2011). For simulated vegetation height, we used the 90th percentile of all woody plants in a grid cell. We calculated the coefficient of variation of biomass and height in each grid cell and for each RCP as a proxy for uncertainty.

All remote sensing products were re-sampled to match the 1° spatial resolution used in simulations. For re-sampling, we used averaging, to account for variation of high-resolution benchmarking data within 1° grid cells.

## 2.7 | Biomass and height changes

To identify areas with substantial changes in woody biomass,  $C_3$  and  $C_4$  grass biomass and vegetation height, we calculated

percentage changes in these variables between current (2019) and future (2099) conditions in each grid cell. For vegetation height, we used the 90th percentile of all woody plants simulated in a grid cell. We tracked if these four state variables changed by more than  $\pm 5\%$ ,  $\pm 10\%$ , ...,  $\pm 50\%$ , and we distinguished between increasing or decreasing trends. Otherwise, biomass or height was classified as stable. We conducted this analysis for the ensemble means of biomass and height of both RCPs. We only provided results for the  $\pm 10\%$  and the  $\pm 50\%$  threshold to represent high and low sensitivity to vegetation change.

## 2.8 | Cultivated and managed vegetation

Large areas in tropical Asia have been converted to cropland and plantations for food and timber production, and have been affected by urbanization, pollution and anthropogenic fire. To account for land use, we overlaid aDGVM2 results with a map of current anthropogenic impact derived from Tuanmu and Jetz (2014), a consensus land-cover product aggregated from four different land-cover products. Specifically, we used 'cultivated and managed vegetation' (class 7) and 'Urban/Built-up' (class 9) of Tuanmu and Jetz (2014; Figure S2).

To account for anthropogenic impacts in benchmarking (Section 2.6), we masked out areas with more than 50% anthropogenic cover fraction. Kumar, Pfeiffer, Gaillard, Langan, and Scheiter (2020) used a similar approach and found that data-model agreement improved for South Asia. To account for anthropogenic impacts in the assessment of biome and phenology transitions, we overlaid areas where aDGVM2 simulates transitions in natural vegetation with the grid cell's anthropogenic cover fraction. Specifically, we multiplied consensus maps indicating areas with (value = 1) or without (value = 0) vegetation change by the fraction

of natural land (i.e. fraction of land not utilized). Values close to 1 indicate areas with a high fractional cover of natural vegetation that is highly susceptible to climate change. Values close to 0 indicate areas without simulated vegetation change or with high fractional cover of utilized land.

As we focused on natural vegetation, our approach does not account for past or future changes in land use, but only for recent land use as represented in the Tuanmu and Jetz (2014) data set. We also ignored impacts of past land use on growth, biomass or vegetation structure in simulations. Local-scale anthropogenic impacts, such as cattle farming, anthropogenic fire, fuelwood harvesting, deforestation or agriculture, were ignored in vegetation simulations. Yet, these impacts are widespread in the study region, and some of them have already been implemented in aDGVM and aDGVM2 (Pfeiffer et al., 2019; Scheiter, Higgins, Beringer, & Hutley, 2015; Scheiter & Savadogo, 2016; Scheiter et al., 2019).

The Tuanmu and Jetz (2014) data set is provided at a 30-arc second spatial resolution, and we aggregated the data to the  $1^\circ$  resolution used in simulations. We summed the respective areas occupied by different classes, and then re-converted the areas to fractions based on the grid cell area size of the  $1^\circ$  resolution used in simulations.

## 3 | RESULTS

### 3.1 | Vegetation state under current climate conditions

Large-scale patterns of simulated aboveground biomass and vegetation height in 2019 showed agreement with remotely sensed biomass and height (Figure 1; Figure S3), indicating that aDGVM2 captured the main features of vegetation in tropical Asia. However,

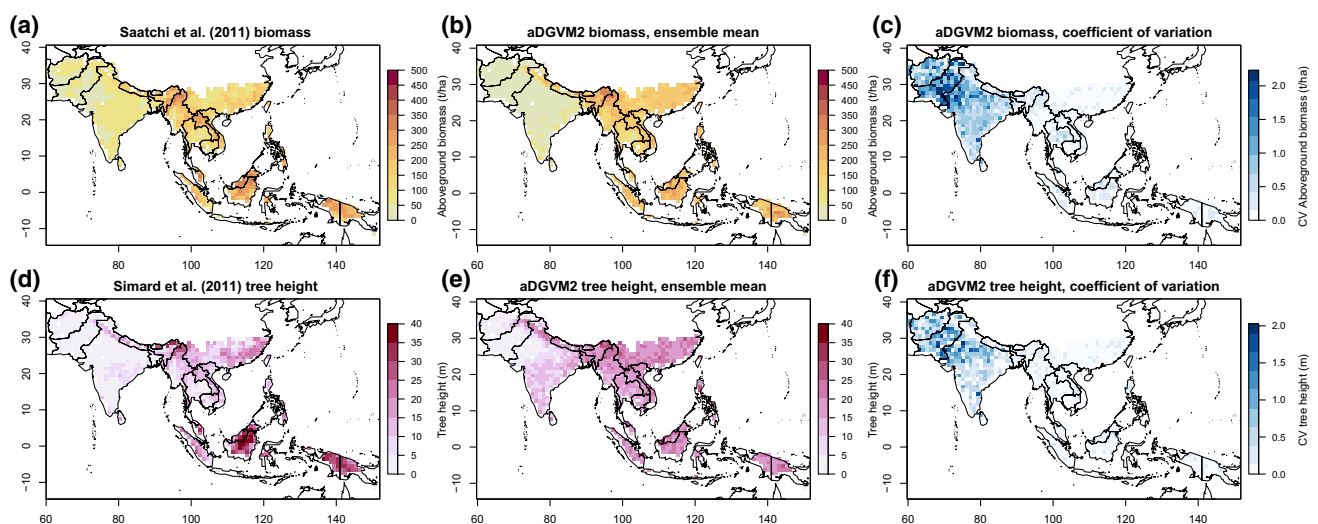


**FIGURE 1** Biomass (a–c) and tree height (d–f) derived from remote sensing (a, d; Saatchi et al., 2011; Simard et al., 2011) and simulated by adaptive dynamic global vegetation model version 2 (aDGVM2) under current conditions (b, e, year 2019). Panels (c, f) show model uncertainty, represented by the coefficient of variation. For aboveground biomass and height, we calculated mean and coefficient of variation for the ensemble of five different general circulation models for RCP8.5. Vegetation height of an ensemble member is represented by the 90th percentile of all woody plants. Results for RCP4.5 are provided in Figure S3. RCP, representative concentration pathway



simulated aboveground biomass and height were lower than observations, primarily on the Indian peninsula. Land use is intense in this region (Figures S2, S4, S5), and explains data-model disagreement. Kumar, Pfeiffer, Gaillard, Langan, and Scheiter (2020) showed that excluding utilized areas for benchmarking improves data-model agreement.

In model simulations, Myanmar, Thailand, Cambodia and most of the Indian peninsula showed both deciduous and evergreen vegetation (Figure 2a; Figure S6a). Phenology in these areas was mostly triggered by water (Figure 2c; Figure S6c). Pakistan was covered by short woody vegetation, and Afghanistan by grasslands and short deciduous vegetation. Phenology was mostly water-triggered with small areas of light-triggered phenology. The mountainous areas of India, the eastern parts of mainland Southeast Asia, tropical China and the islands of Indonesia, the Philippines and New Guinea were covered by tall evergreen vegetation (Figure 2a; Figure S6a), and phenology was triggered by both water and light (Figure 2c; Figure S6c).

Model results for different RCPs and GCMs varied considerably. We found variation between ensemble members with respect to the area covered by different biomes, and between ensemble members and the consensus maps of all ensemble members (Table 1; Table S1). For instance, in the ensemble mean for RCP4.5, 55.3% of the area was covered by the tall evergreen biome type under current conditions with a range between 44.3% for GFDL-ESM2M and 58.2%

for MIROC-ESM. Mean aboveground biomass varied between ensemble members (Table 2) and ranged between 122.0 t/ha for IPSL-CM5A-LR and 143.7 t/ha for MIROC-ESM in RCP4.5, with an ensemble mean of 131.9 t/ha for 2000–2019.

For both aboveground biomass and vegetation height, the coefficient of variation of ensemble members was highest in more arid and seasonal areas with short vegetation (Figure 1c,f; Figure S3c,f). With respect to biome types, we found high agreement between ensemble members in areas covered by tall evergreen vegetation, while in areas covered by deciduous vegetation, agreement was typically lower (Figure 2b; Figure S6b). The dominant phenological type showed less large-scale areas of agreement than biome type (Figure 2d; Figure S6d).

### 3.2 | Climate change impacts on biomass and height

Under future climate change, aboveground biomass in the study area showed substantial increases for both RCPs (Figure 3a; Table 2). In RCP4.5, ensemble mean aboveground biomass in the entire study region increased from 121.1 t/ha in the historic period (1950–1969) to 131.9 t/ha under current conditions (2000–2019), and to 148.7 t/ha under future conditions (2080–2099), representing a 22.8% increase between historic and future conditions and

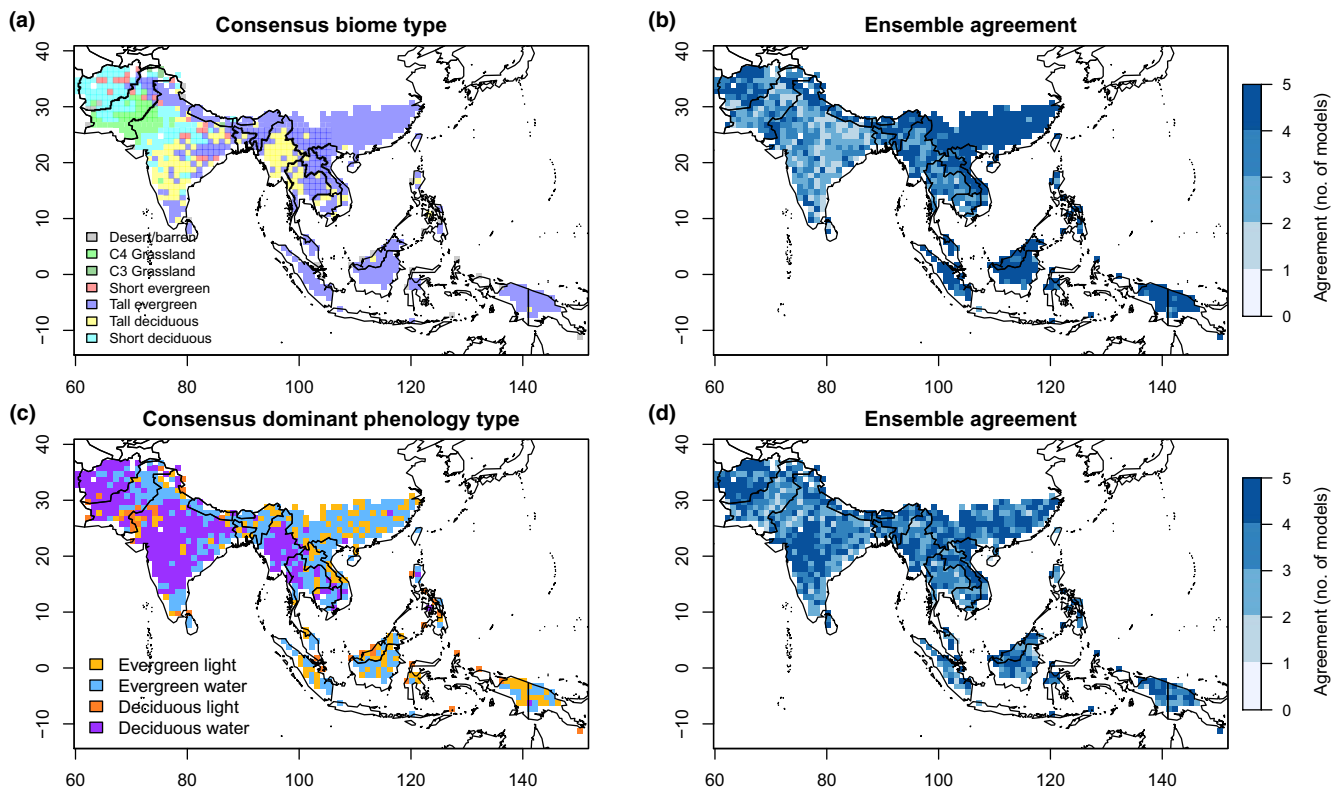


**FIGURE 2** Consensus biome types (a) and dominant phenology types (c) simulated by adaptive dynamic global vegetation model version 2 under current conditions (year 2019). Panels (a, c) show consensus maps, (b, d) show uncertainty, represented by the number of ensemble members that simulate the consensus type. Simulations were conducted for RCP8.5. Results for RCP4.5 are provided in Figure S6. RCP, representative concentration pathway

**TABLE 1** Cover of different biome types for current (2019) and future (2099) climate conditions for RCP4.5 and RCP8.5. Cover is provided as percentage of grid cells covered by different biomes. Cover fractions for all ensemble members and the ensemble mean are provided. Values for current conditions are provided two times, because simulations for RCP4.5 and RCP8.5 slightly diverge due to model stochasticity and differences in the climate data sets. Models: 'M1' GFDL-ESM2M; 'M2' HadGEM2-ES; 'M3' IPSL-CM5A-LR; 'M4' MIROC-ESM; 'M5' NorESM1-M; 'Ens' ensemble mean. Table S1 provides cover fractions for biomes aggregated by height or phenology

Biome	Time	RCP	M1	M2	M3	M4	M5	Ens
Desert	Current	4.5	5.5	2.7	3.0	2.7	2.8	2.7
	Future	4.5	3.9	3.0	4.1	2.7	3.0	2.8
	Current	8.5	4.6	2.7	3.1	3.0	3.2	3.1
	Future	8.5	4.8	3.0	3.6	3.0	2.8	2.8
C <sub>4</sub> grassland	Current	4.5	4.6	8.9	6.4	9.2	6.4	7.2
	Future	4.5	6.2	8.2	6.1	8.6	6.4	7.3
	Current	8.5	5.7	8.8	6.0	8.6	6.6	7.2
	Future	8.5	4.7	7.8	5.7	7.1	6.3	6.4
C <sub>3</sub> grassland	Current	4.5	1.0	0.9	0.2	1.0	1.1	0.6
	Future	4.5	0.7	0.7	1.1	0.7	0.9	0.6
	Current	8.5	0.6	0.9	1.1	0.9	1.0	0.5
	Future	8.5	0.7	0.6	0.9	1.0	0.6	0.7
Short deciduous	Current	4.5	14.8	15.3	18.9	9.3	15.3	15.7
	Future	4.5	12.5	13.2	16.4	8.7	12.3	12.4
	Current	8.5	14.6	15.7	18.3	9.7	14.6	14.7
	Future	8.5	13.6	12.5	16.5	8.4	11.9	12.6
Tall deciduous	Current	4.5	28.0	12.6	14.2	14.6	13.0	15.8
	Future	4.5	29.3	12.1	15.7	15.2	15.8	18.2
	Current	8.5	28.8	11.5	13.7	14.3	13.2	15.9
	Future	8.5	28.0	12.5	14.9	16.3	16.4	17.7
Short evergreen	Current	4.5	1.9	4.4	4.6	5.1	3.3	2.7
	Future	4.5	1.4	4.7	2.9	3.0	2.1	1.4
	Current	8.5	1.7	4.1	4.7	4.3	3.5	2.8
	Future	8.5	1.1	4.2	2.9	2.9	1.9	1.7
Tall evergreen	Current	4.5	44.3	55.1	52.7	58.2	58.0	55.3
	Future	4.5	46.0	58.1	53.7	61.1	59.5	57.4
	Current	8.5	43.9	56.3	53.1	59.4	57.9	55.7
	Future	8.5	46.9	59.5	55.5	61.4	60.1	58.0

Abbreviation: RCP, representative concentration pathway.

12.7% between current and future conditions (Table 2). In RCP8.5, aboveground biomass increased to 163.0 t/ha in the future period (2080–2099), representing an increase of 34.8% between historic and future conditions and an increase of 22.8% between current and future conditions (Table 2). Trend lines of interannual biomass change between consecutive years showed an increase until the 2040s in both RCP4.5 and RCP8.5. However, while interannual biomass change then decreased until 2099 in RCP4.5, it remained stable in RCP8.5 (Figure 3b). When averaged for the entire study period and all ensemble members, biomass changed by  $0.29 \pm 1.66$  t/ha in RCP8.5 and  $0.19 \pm 1.74$  t/ha in RCP4.5 between consecutive years (Figure 4).

In RCP8.5, aboveground biomass changes by more than 10% between current and future climate were simulated in almost the

entire study region, except for areas in tropical China (Figure 5a; Figure S10a–c). Vegetation height changed more than 10% in South Asia and western mainland Southeast Asia and less than 10% in areas where the model simulated tall vegetation under current conditions (Figure 5b; Figure S10d–f). Decreases in aboveground biomass and height were only detected in Pakistan and Afghanistan (Figure 5b). C<sub>3</sub> aboveground grass biomass showed decreases in the entire study region, except in Pakistan and Afghanistan (Figure 5c), where C<sub>3</sub> aboveground grass biomass was low (Figure S10g–i). C<sub>4</sub> grass biomass increased primarily in areas currently covered by deciduous vegetation and decreased in areas covered by evergreen vegetation (Figure 5d; Figure S10j–l). The area affected by changes was smaller when a 50% threshold was used to detect changes (Figures S8, S9).

**TABLE 2** Aboveground vegetation biomass in the study region for different GCMs and RCPs and changes between different time periods (historic: 1950–1969; current: 2000–2019; future: 2080–2099). Biomass values for each ensemble member and the ensemble mean are provided. Models: 'M1' GFDL-ESM2M; 'M2' HadGEM2-ES; 'M3' IPSL-CM5A-LR; 'M4' MIROC-ESM; 'M5' NorESM1-M; 'Ens' ensemble mean;  $\Delta$  indicates percentage aboveground biomass changes between time periods

Time	RCP	M1	M2	M3	M4	M5	Ens
Historic (t/ha)	4.5	117.8	116.5	112.0	133.8	125.2	121.1
Current (t/ha)	4.5	125.1	128.9	122.0	143.7	140.0	131.9
Future (t/ha)	4.5	145.7	142.8	134.4	159.0	161.7	148.7
$\Delta$ Historic to current (%)	4.5	6.2	10.6	8.9	7.4	11.8	8.9
$\Delta$ Current to future (%)	4.5	16.5	10.8	10.2	10.6	15.5	12.7
$\Delta$ Historic to future (%)	4.5	23.7	22.6	20.0	18.8	29.2	22.8
Historic (t/ha)	8.5	118.0	116.1	111.2	134.3	124.7	120.9
Current (t/ha)	8.5	126.4	129.9	121.2	148.2	137.8	132.7
Future (t/ha)	8.5	159.1	156.6	142.9	179.1	177.7	163.0
$\Delta$ Historic to current (%)	8.5	7.1	11.9	9.0	10.3	10.5	9.8
$\Delta$ Current to future (%)	8.5	25.9	20.6	17.9	20.9	28.7	22.8
$\Delta$ Historic to future (%)	8.5	34.8	34.9	28.5	33.4	42.3	34.8

Abbreviations: GCM, general circulation model; RCP, representative concentration pathway.

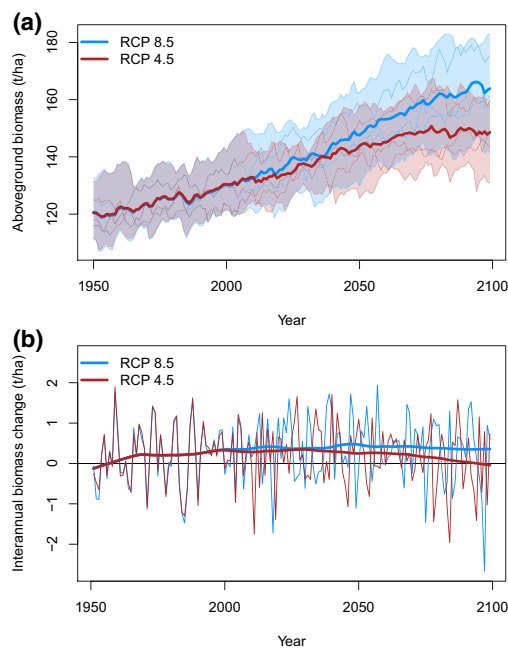


**FIGURE 3** Aboveground vegetation biomass (a) and interannual biomass change between consecutive years (b) in model ensemble between 1950 and 2099 for tropical Asia. Thin lines in panel (a) represent mean annual aboveground biomass in simulations with different general circulation models, bold lines represent annual ensemble means for RCP4.5 and RCP8.5, and shaded areas represent the range (minimum and maximum) of the ensemble in both RCPs. Thin lines in panel (b) represent ensemble means, thick lines represent smoothed lines using 'lowess'. RCP, representative concentration pathway

The broad patterns of change in aboveground biomass and vegetation height in RCP4.5 were similar to the patterns in RCP8.5, yet the areas of increase were smaller (primarily in tropical China)

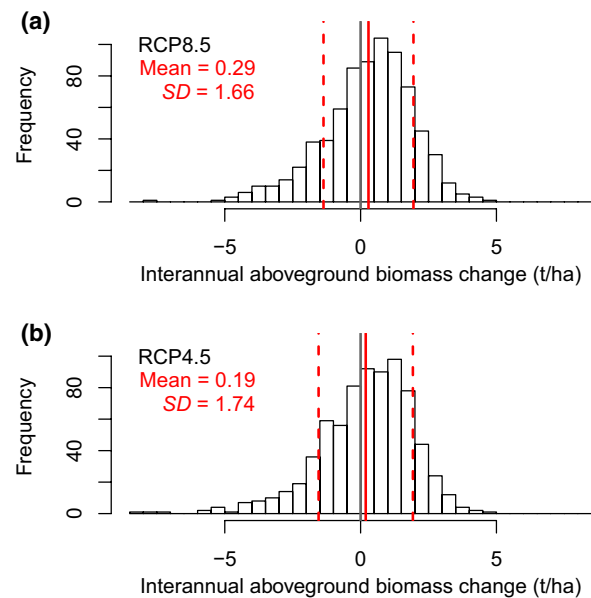


**FIGURE 4** Histograms of interannual aboveground biomass change between two consecutive years for (a) RCP8.5 and (b) RCP4.5. Histograms were plotted for all years between 1950 and 2099 for all ensemble members. The solid red line indicates the average of all changes, the dashed red lines indicate standard deviation. Time series of ensemble means of these changes are provided in Figure 3b. RCP, representative concentration pathway

while the areas of decrease were larger (primarily in Pakistan and Afghanistan, Figures S7, S11).

Variation in absolute aboveground biomass and biomass change between different ensemble members was substantial between 1950 and 2099 (Table 2). In RCP8.5, mean aboveground biomass in the study region ranged between 142.9 t/ha for ISPL-CM5A-LR and 179.1 t/ha for MIROC-ESM in 2099. Biomass change



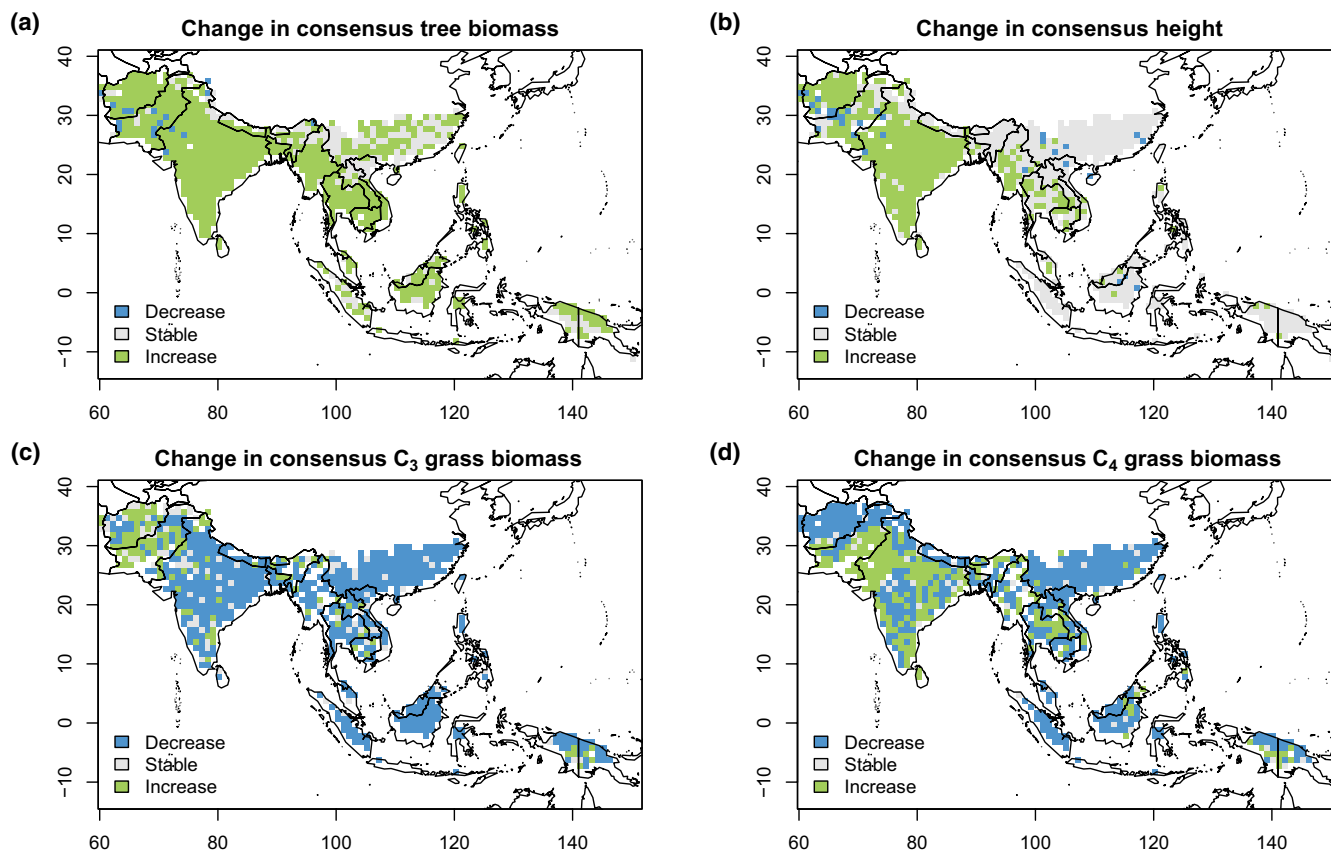


**FIGURE 5** Areas where aboveground tree biomass and height change by more than  $\pm 10\%$  between current (year 2019) and future (year 2099) conditions in RCP8.5. For biomass, we used tree aboveground biomass (a), C<sub>3</sub> grass biomass (c) and C<sub>4</sub> grass biomass (d) in a grid cell, for vegetation height (b), we used the 90th percentile of all trees simulated in a grid cell. Results for RCP4.5 are provided in Figure S7. RCP, representative concentration pathway

between current and future conditions ranged between 10.2% (IPSL-CM5A-LR) and 16.5% (GFDL-ESM2M1) for RCP4.5, and between 17.9% (IPSL-CM5A-LR) and 28.7% (NorESM1-M) for RCP8.5 (Table 2).

### 3.3 | Climate change impacts on phenology and biomes

The aDGVM2 simulated changes in community composition under future climate conditions, specifically regarding the abundances of deciduous and evergreen vegetation (Figure 6). In RCP8.5, we found increases in the abundance of light-triggered (Figure 6a–c) and water-triggered (Figure 6d–f) evergreen plants and decreases in the abundance of water-triggered deciduous plants in mainland Southeast Asia, central India and Pakistan (Figure 6g–i). In southern India, water-triggered evergreen plants decreased to the benefit of deciduous water-triggered plants. Similar patterns were simulated for RCP4.5 (Figure S12).

Changes in aboveground woody biomass and the abundances of phenological types caused biome transitions, predominantly from small to tall, and from deciduous to evergreen biome types (Figure 7a,b; Figure S13a,b). This trend was most pronounced in

India and mainland Southeast Asia. Vegetation on the islands was stable, that is, aDGVM2 simulated tall evergreen vegetation for all ensemble members and time periods. The area affected by biome transitions varied within the ensemble (Table 1; Table S1). In the consensus biome map, aDGVM2 simulated biome transitions for 8.4% of the study region in RCP4.5 and 8.3% in RCP8.5, with values ranging between 7.9% and 10.0% among ensemble members (Table 3; Figure 7c). The area where at least one ensemble member projected a biome transition between current and future conditions was larger and 28.5% for RCP4.5 and 30.4% for RCP8.5, respectively (Table 3; Figure 7d). These areas covered most of India and Pakistan and large areas in mainland Southeast Asia.

When cultivated and managed land was considered (Figure S2; Tuanmu & Jetz, 2014), areas that were subject to biome transitions were smaller. These areas include grasslands and short vegetation in the west of the study region, tall vegetation in the east of the Indian peninsula and tall vegetation in mainland Southeast Asia (Figure 7e,f; Figure S13e,f).

Despite changes in the abundances of phenological strategies, we found that patterns of dominant phenological types were more stable between current and future climate conditions than the patterns of state variables and biome types (Figure 8;

**FIGURE 6** Relative abundance of different phenological strategies under current (year 2019) and future (year 2099) conditions, as well as change within this time period. Phenological strategies are evergreen light-triggered (a–c), evergreen water-triggered (d–f), deciduous water-triggered (g–i) and deciduous light-triggered (j–l). Simulations for current conditions (a, d, g, j), future conditions (b, e, h, k) and changes between current and future conditions (c, f, i, l) are provided. The maps show ensemble means for RCP8.5. Results for RCP4.5 are provided in Figure S12. RCP, representative concentration pathway

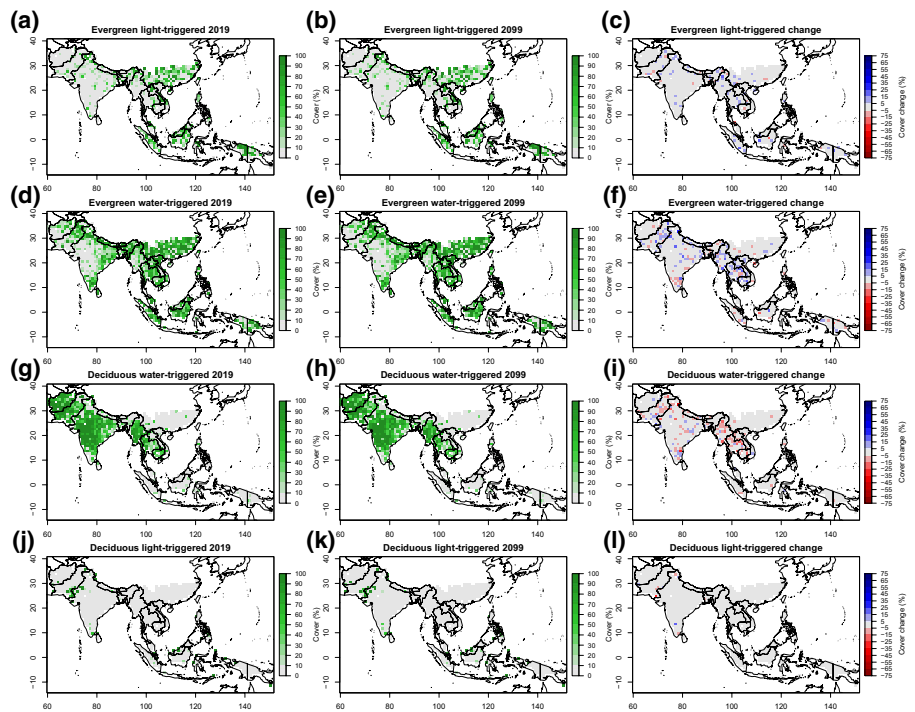


**FIGURE 7** Consensus map of current (a, year 2019) and future (b, 2099) biome distribution in RCP8.5 for the ensemble. Areas where biome shifts between 2019 and 2099 were simulated for the consensus map (c, e) and in at least one of the ensemble members (d, f) are highlighted without land use impacts (c, d) and with land use impacts (e, f). Land use was derived from Tuanmu and Jetz (2014). Results for RCP4.5 are provided in Figure S13. RCP, representative concentration pathway

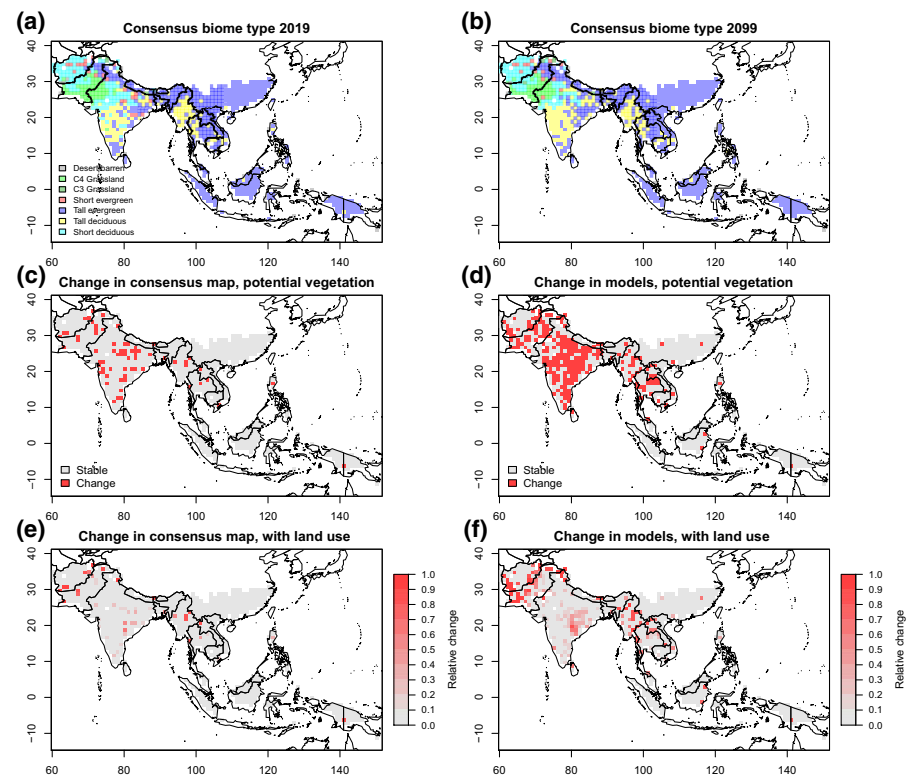


Figure S14). In the consensus map, only 2.7% and 3.5% of the simulated grid cells showed changes in the dominant phenological type in RCP4.5 and RCP8.5 respectively (Table 3). Values in ensemble members ranged between 1.7% and 5.0%. Phenology changes in at least one ensemble member were predicted for 13.4% of the study area in RCP4.5 and 15.8% in RCP8.5. The most frequent type of phenology change was from deciduous

water-triggered to evergreen water-triggered phenology, and these changes were mostly projected in warm areas with intermediate mean annual precipitation between ca. 500 mm and 2,000 mm (Figure 9; Figure S15). Masking of cultivated and managed land (Figure S2; Tuanmu & Jetz, 2014) reduced the area where transitions in dominant phenology occurred (Figure 8e,f; Figure S14e,f).

**TABLE 3** Percentage of simulated grid cells in tropical Asia affected by transitions in biome type and in dominant phenology type for different GCMs and RCPs. Changes represent the period between current (year 2019) and future (year 2099) conditions. Models: 'M1' GFDL-ESM2M; 'M2' HadGEM2-ES; 'M3' IPSL-CM5A-LR; 'M4' MIROC-ESM; 'M5' NorESM1-M; 'Ens' ensemble mean; 'Ova' overall change of all GCMs, that is, area where at least one GCM simulates a transition

	RCP	M1	M2	M3	M4	M5	Ens	Ova
Biome type	4.5	8.2	8.0	10.0	7.9	8.3	8.4	28.5
Biome type	8.5	8.1	9.3	9.5	9.2	9.9	8.3	30.4
Phenology	4.5	2.9	3.6	1.7	3.1	3.6	2.7	13.4
Phenology	8.5	3.5	3.6	1.9	5.0	3.5	3.5	15.8

Abbreviations: GCM, general circulation model; RCP, representative concentration pathway.

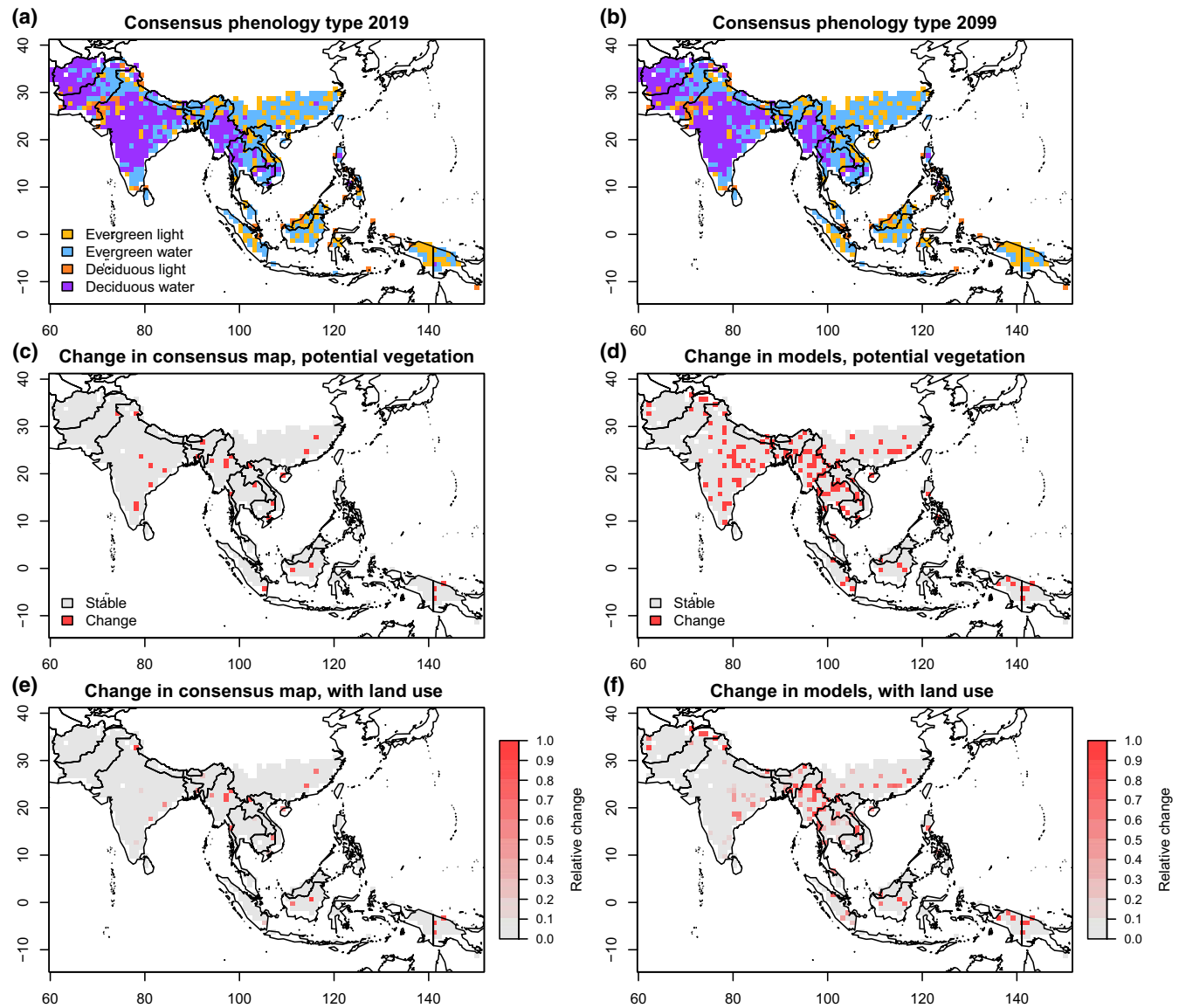


**FIGURE 8** Consensus map of current (a, year 2019) and future (b, 2099) distribution of dominant phenological types in RCP8.5 for the ensemble. Areas where phenology shifts between 2019 and 2099 were simulated for the consensus map (c, e) and in at least one of the ensemble members (d, f) are highlighted without land use impacts (c, d) and with land use impacts (e, f). Land use was derived from Tuanmu and Jetz (2014). Results for RCP4.5 are provided in Figure S14. RCP, representative concentration pathway

In the ensemble mean, transpiration showed a decrease of approximately 4% between 1950 and current conditions (Figure S16), despite increases in aboveground biomass. In RCP4.5, aDGVM2

simulated increases of transpiration to values similar to 1950 by the end of the century. In contrast, transpiration stabilized at the reduced value in RCP8.5.

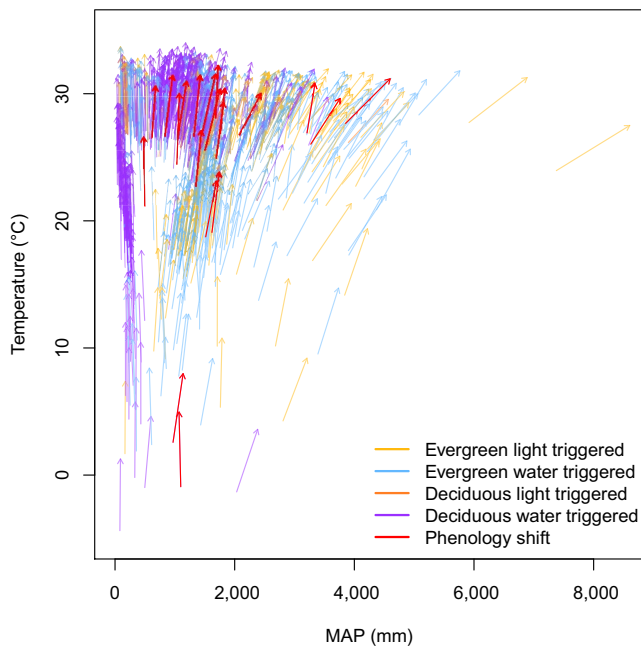


**FIGURE 9** Transitions of dominant phenology in precipitation-temperature space for the RCP8.5 ensemble. Origin and end of arrows indicate location of a grid cell in climate space in 2019 and 2099; colours indicate different dominant phenological strategies and if a transition in the phenology was projected (red arrows) or not (other colours). Results for RCP4.5 are provided in Figure S15. MAP, mean annual precipitation; RCP, representative concentration pathway

## 4 | DISCUSSION

### 4.1 | Biomass increase and CO<sub>2</sub> fertilization

Previous modelling and remote sensing studies have shown increased vegetation productivity (Haverd et al., 2020) and greening trends (Piao et al., 2020) globally, and that the biosphere has acted as a carbon sink during recent decades (Le Quere et al., 2018; Liu et al., 2019). Model simulations with aDGVM2 also showed increases in aboveground vegetation biomass for historic and future periods, indicating that regions covered by natural vegetation will remain a carbon sink until 2099. This trend was robust for an ensemble of two climate change scenarios and five GCMs. In RCP8.5, trends of interannual biomass changes between consecutive years remained almost constant until 2099, indicating that the carbon uptake rate and the sink potential of natural vegetation remain stable. In contrast, in RCP4.5 interannual biomass change decreased between the 2030s and 2099. This result agrees with Hubau et al. (2020), who found sink saturation in tropical forests in Africa and Amazonia. However, our results indicate later saturation in RCP4.5 than reported by Hubau et al. (2020). In most of our study area, aboveground woody biomass increase exceeded 10%. Exceptions were found for some patches of evergreen forest in tropical China and the islands of Indonesia, Malaysia, the Philippines and New Guinea, where aboveground biomass was already high under current climate conditions. Biomass decreases exceeding 10% occurred only in arid areas with low aboveground biomass.

Simulated aboveground woody biomass increase is, in aDGVM2, primarily driven by CO<sub>2</sub> fertilization effects of plant growth. We already found and quantified CO<sub>2</sub> fertilization in the predecessor model version aDGVM (Higgins & Scheiter, 2012; Martens et al., under review; Scheiter & Higgins, 2009; Scheiter et al., 2015). Kumar, Pfeiffer, Gaillard, Langan, and Scheiter (2020) and Langan (2019) confirmed CO<sub>2</sub> fertilization effects for aDGVM2 for South Asia and Amazonia, respectively, by conducting simulations with CO<sub>2</sub> fertilization effects enabled or disabled.

Several lines of empirical evidence support these modelled effects of elevated CO<sub>2</sub> on vegetation. First, open-top chamber experiments in different ecosystems showed increases in photosynthetic rates and water use efficiency at leaf or plant level (Kgope, Bond, & Midgley, 2010; B. S. Ripley and S. Raubenheimer, personal communication, March 2019). Free air carbon enrichment (FACE) experiments in different ecosystems revealed ecosystem-level responses to elevated CO<sub>2</sub>. Ecosystem responses were ecosystem-specific (Hickler, Rammig, & Werner, 2015) and variable over time, often with strong responses at the beginning of eCO<sub>2</sub> treatments but weaker long-term responses. CO<sub>2</sub> enrichment experiments in the study region are scarce. Deng et al. (2010) and Liu et al. (2008) used open-top chambers to study soil respiration and nutrient dynamics in tropical forests in China. FACE experiments are currently missing in the study region, and there is an urgent need for such experiments.

Second, greening trends have been observed in tropical Asia and globally during recent decades (Piao et al., 2020). These have been attributed, among other drivers, to elevated CO<sub>2</sub>. Haverd et al. (2020) attributed 30% of the increase in gross primary productivity since 1990 to CO<sub>2</sub> fertilization. Piao et al. (2015) used satellite-derived leaf area index (LAI) and modelling techniques to show greening trends in China, and identified elevated CO<sub>2</sub> and nitrogen deposition as the most likely drivers. Yet, Piao et al. (2015) also included anthropogenic afforestation as a factor driving greening, and not only natural vegetation dynamics. Greening is typically quantified by remotely sensed indicators such as the normalized difference vegetation index or LAI. These indicators are proxies for leaf biomass and leaf productivity, but do not necessarily imply increases in carbon sequestration or sink potential. Chen et al. (2019) argued that increases in LAI and CO<sub>2</sub> fertilization accounted for 12.4% and 47% of the terrestrial carbon sink since 1981, respectively, indicating links between greening and carbon sequestration.

Third, woody encroachment is observed in many savanna regions globally (Stevens, Lehmann, Murphy, & Durigan, 2017). In South African savannas, encroachment has often been attributed to CO<sub>2</sub> fertilization (Buitenwerf, Bond, Stevens, & Trollope, 2012; Kgope et al., 2010). Woody encroachment has also been observed in Indian savannas and the central dry zone of Myanmar, where alien shrub species such as *Lantana camara*, *Chromolaena odorata* and *Prosopis juliflora* rapidly invade native vegetation (Hiremath & Sundaram, 2005; Kannan, Shackleton, & Uma Shaanker, 2013; Oo & Koike, 2015; Ratnam et al., 2016). These studies attributed encroachment to

anthropogenic activities such as fire suppression or overgrazing rather than to elevated  $\text{CO}_2$ . It remains to be tested to what degree  $\text{CO}_2$  effects reinforce other anthropogenic impacts or drive encroachment. Generally,  $\text{CO}_2$ -induced woody encroachment has been less studied in tropical Asia than in southern Africa (e.g. Bond, 2008; Bond, Midgley, & Woodward, 2003; Buitenwerf et al., 2012; Midgley & Bond, 2015). One explanation for the lack of study is that tropical Asia has a higher human population than other tropical regions. Human impacts associated with deforestation, or conversion of natural vegetation to cropland may override any  $\text{CO}_2$  or climate change effects on vegetation. Further, Asian savannas are often misinterpreted as degraded forest and management policies aim at afforestation rather than at the conservation of these landscapes (Kumar, Pfeiffer, Gaillard, Langan, Martens, et al., 2020; Ratnam et al., 2016). In this context, woody encroachment might be interpreted as a desired transitional stage towards forest expansion and as successful afforestation, rather than as a threat to biodiversity.

Our results largely agree with previous DGVM studies for tropical Asia that reported greening under future climate conditions. For instance, Sitch et al. (2008) compared different DGVMs for IPCC SRES A1F1 and showed that the models simulate stability or increases in vegetation carbon and woody cover in tropical Asia between 1860 and 2100. Yu, Wang, Parr, and Ahmed (2014) analysed a global ensemble run for RCP8.5 with 19 GCMs using CLM-CN-DV and found that net primary productivity is likely to increase in tropical Asia until the end of the century. Woody vegetation cover was projected to increase in most of the study area, except along the Himalayas and northern Indonesia (Yu et al., 2014). Using aDGVM, the predecessor of aDGVM2, we simulated substantial transitions from grasslands to savannas and from savannas to forests until 2100 in South Asia (Kumar & Scheiter, 2019).

While simulated aboveground biomass and vegetation height reflected broad patterns of remote sensing data, we also found areas where data and model disagree. For example, aDGVM2 underestimates biomass and height in areas highly affected by land use, such as the Indian peninsula. Further, aDGVM2 does not simulate some of the *dipterocarp* forests, with biomass of more than 400 t/ha and giant trees which can exceed 70 m in height and store large biomass. This mismatch can be explained by aDGVM2 not representing such giant trees, and by the coarse resolution of aDGVM2 simulations that ignores observed spatial heterogeneity. Conducting higher resolution simulations and replicate runs for model grid cells might capture heterogeneity and extremes of biomass and height at local scale. However, we expect that such additional simulations would not influence our general results.

## 4.2 | Ecological strategies, biomes and ecosystem functions

The community assembly processes implemented in aDGVM2 allow the simulation of a diversity of distinct ecological strategies at local scale, as well as their responses to climate change (Langan

et al., 2017; Scheiter et al., 2013). Thus, simulated vegetation at local scale was characterized by the coexistence of deciduous and evergreen plants, water- and light-triggered plants, single-stemmed trees and multi-stemmed shrubs, small and tall plants, as well as grasses and woody plants. The aDGVM2 selected for high grass biomass and dominance of water-triggered deciduous woody plants on the Indian peninsula, Pakistan and Afghanistan, and for tall evergreen woody vegetation in tropical China, the islands of Indonesia, the Philippines and New Guinea, as well as in the Himalayas. Interestingly, aDGVM2 simulated a mixture of light- and water-triggered phenology in most of the tall evergreen biomes of southern China, mainland Southeast Asia and the islands. We explain this mixture by high resource availability. While light-triggered evergreen plants are filtered out in more arid and seasonal regions, they can persist and coexist with water-triggered evergreen plants if water availability is high. Whether plants are triggered by water or light might not have substantial impacts on vegetation dynamics and ecosystem functions in these areas.

A representation of vegetation as a mixture of various ecological strategies with overlapping climatic envelopes in aDGVM2 agrees with reality. For instance, distributions of  $\text{C}_3$  and  $\text{C}_4$  grasses typically overlap rather than being disjoint (Still, Berry, Collatz, & DeFries, 2003). Ge and Xie (2017) found overlapping distributions of evergreen and deciduous trees in tropical China, and open woody ecosystems such as savannas are mixtures of grasses, shrubs and trees (Ratnam et al., 2011, 2016), ranging from low to high tree cover (Sankaran et al., 2005).

Our simulations revealed climate change impacts on the relative abundance of different ecological strategies, the biome type and the dominant phenological type. As expected, aDGVM2 mainly simulated transitions from small to tall biome types and from deciduous to evergreen biome types. Changes in height structure can be explained by  $\text{CO}_2$  fertilization and associated increases in growth rates and aboveground biomass of woody plants. Changes in phenology from water-triggered to light-triggered types can be explained by increasing precipitation and reduced transpirational demand in  $\text{C}_3$  plants (Figure S16). A meta-analysis by Soh et al. (2019) showed that increases in intrinsic water use efficiency in response to elevated  $\text{CO}_2$  are higher in evergreen plants than in deciduous plants, which may explain a relative advantage of evergreen plants over deciduous plants under elevated  $\text{CO}_2$  in aDGVM2. Phenology of simulated vegetation in the Himalayas was predominantly evergreen (Ralhan, Khanna, Singh, & Singh, 1985) and not influenced by climate change. Whether future temperature increase will influence phenology in these regions remains unclear as temperature does not directly trigger phenology in aDGVM2. Temperature may influence phenological strategies indirectly via impacts on the carbon balance and mortality and associated selection for certain strategies. Predictive understanding of plant phenology is still challenging. Further model development is required to integrate triggers such as water, temperature, nutrients, radiation or day length (Adole, Dash, & Atkinson, 2018; Piao et al., 2019), for example to account for the effects of temperature increase on phenology and growing season length in alpine



vegetation in the Himalayas, or to predict widely observed pre-rain greening (Adole et al., 2018).

Transitions from deciduous to evergreen vegetation simulated by aDGVM2 agree with previous modelling studies. Ravindranath et al. (2006) used the BIOME4 model to simulate the responses of Indian forest to SRES A2 and B2 simulated by the Hadley Centre model (HadRM3). In addition to changes towards evergreen phenology, their study reported increases in savanna vegetation and decreases in more xeric vegetation types. The effects were attributed to CO<sub>2</sub> fertilization and associated increases in net primary productivity (Ravindranath et al., 2006). Chaturvedi et al. (2011) found transitions towards evergreen forests using the IBIS model.

Modelled transition rates of biomes and dominant phenology types might be overestimated compared to real transition rates. While it has been shown that species and biomes might not be able to keep pace with climate change (Loarie et al., 2009; Scheiter, Moncrieff, Pfeiffer, & Higgins, 2020), most DGVMs ignore seed dispersal and associated migration lags (Corlett & Westcott, 2013). Models assume that local seed pools contain all functional types or ecological strategies that persisted during model spin-up, and that climate change or other disturbances influence the relative abundance of these types. This modelling approach represents an establishment bottleneck that prevents or delays invasion of inferior ecological strategies or functional types into local communities, but at the same time it represents a full dispersal scenario (Thuiller, Lavorel, Araujo, Sykes, & Prentice, 2005). While this caveat is well known (Blanco et al., 2014; Corlett, 2009; Corlett & Westcott, 2013; Scheiter et al., 2020), it has rarely been addressed in DGVMs (but see Sato & Ise, 2012). Reasons include the mismatch between the coarse resolution of DGVM studies (typically 0.5° or coarser) and shorter dispersal distances, and knowledge gaps about dispersal distances, probabilities and pathways (Corlett, 2009). Modelling dispersal and migration is particularly challenging in highly fragmented and heterogeneous landscapes (Nabel, Zurbiggen, & Lischke, 2013) such as the Himalayas or the islands of tropical Asia.

### 4.3 | The ensemble approach

Simulated aboveground biomass, vegetation height and biome patterns differed between ensemble members under both current and future climate conditions. These differences can be attributed both to stochastic processes in aDGVM2 that cause differences between model runs even for similar environmental forcing, and to differences between environmental forcing data in the ISIMIP climate data ensemble (Warszawski et al., 2014; Figure S1). Deviation between aDGVM2 ensemble members was higher in more arid regions. In these regions, environmental conditions showed higher interannual variation and stochastic processes in aDGVM2, such as fire occurrence or demographic processes, had a greater effect on vegetation dynamics. This model behaviour confirms a previous aDGVM result indicating that fire-driven and open ecosystems are more variable

and take longer to reach an equilibrium state with prevailing environmental conditions than forest (Scheiter et al., 2020).

Projecting future climate using GCMs, particularly patterns of precipitation, is challenging. Differences between GCMs explain variation in climate data within the ISIMIP ensemble. For instance, simulations of the monsoon and associated variability in precipitation are still uncertain in models. Raghavan, Liu, Nguyen, Vu, and Liong (2018) compared CMIP5 simulations of historical rainfall to observations for Southeast Asia and found that none of the models represented observations particularly well. The benefit of using ensembles of climate change scenarios is therefore that a wide range of potential climate change impacts is covered, and that most likely vegetation changes can be identified.

### 4.4 | Anthropogenic impacts and implications for management

Our results have important implications for management and conservation under climate change. First, we showed that areas in tropical Asia covered by natural vegetation are likely to remain carbon sinks until 2099, when ignoring land use changes. This provides support for forest conservation and restoration as climate change mitigation strategies (Graham, Laurance, Grech, McGregor, & Venter, 2016). However, the carbon sink potential also implies possible transitions from ancient grasslands and savannas into forests, both due to natural processes and due to deliberate afforestation. Transitions to forests may lead to conflicts of interest between stakeholder groups promoting carbon sequestration by afforestation, and those promoting conservation of biodiversity and traditional land use practices in grassland and savanna ecosystems (Bond, Stevens, Midgley, & Lehmann, 2019). Reaching compromises between these interest groups and the resident communities will be challenging but necessary to balance biodiversity conservation against successful climate change mitigation and adaptation.

Second, we found substantial differences between RCPs and GCMs. This underlines that the ensembles of climate scenarios and vegetation models are necessary to cover a wide range of possibilities required for the development of sustainable management strategies. Relying on a single set of climate forcing data may constrain the range of possible vegetation states and lead to inappropriate management decisions. Utilization of regionally adapted vegetation models (Moncrieff, Bond, & Higgins, 2016; Moncrieff, Scheiter, Langan, Trabucco, & Higgins, 2016) and high-resolution climate forcings that capture the local climate phenomena are highly recommended.

Third, our results indicate a trade-off between monitoring past and future vegetation changes by continuous state variables, such as aboveground biomass or tree cover, and classifying vegetation into biomes. The advantage of biome classification is that biomes reflect the status of multiple state variables and the associated ecosystem functions (Higgins et al., 2016; Moncrieff, Bond, et al., 2016; Moncrieff, Scheiter, et al., 2016). Biome transitions indicate

simultaneous changes in multiple features of vegetation. Biomes are a compelling framework to understand large-scale biogeographic patterns, and to communicate model results in an aggregated way. A caveat of using biomes is that biome transitions may suggest fundamental vegetation changes, species turnover or non-linear tipping-point behaviour. In fact, biome transitions might be triggered by smooth and moderate changes in variables used to define biome types.

The advantage of using continuous state variables is that even small changes in the vegetation state can be detected. Such changes might not necessarily modify the biome state but nonetheless influence the vegetation state and ecosystem functions. Keeping track of simultaneous changes in multiple state variables and interpreting the implications for ecosystem functioning might be more difficult than using a biome approach (Conradi et al., 2020). There is no single consensus biome classification scheme that adequately covers all biome types globally (Moncrieff, Bond, et al., 2016; Moncrieff, Scheiter, et al., 2016; Mucina, 2019), and that can be applied in modelling studies, remote sensing and other observational studies. We argue that biome classification schemes should be tailored to specific research questions to ensure that they reflect targeted vegetation states and ecosystem functions. Inappropriate classification of vegetation may misguide decision-making (Kumar, Pfeiffer, Gaillard, Langan, Martens, et al., 2020).

Finally, we showed that areas with deciduous vegetation are most susceptible to climate change. They included grasslands in Afghanistan and Pakistan, as well as deciduous vegetation on the Indian peninsula and in mainland Southeast Asia. However, large proportions of these areas have already been transformed into managed land, and the areas not affected by direct anthropogenic effects are mostly small and scattered. This result highlights an urgent need to conserve and protect remaining patches of natural vegetation that are exposed to both anthropogenic pressure and climate change. Future high-resolution and region-specific modelling studies can help to identify migration corridors for different vegetation types and inform planning of protected areas, human-assisted migration (Corlett, 2009), and the establishment or restoration of habitat connectivity (Corlett & Westcott, 2013), while accounting for climate change impacts on vegetation. Here, we focused on natural vegetation and implications for remaining areas of undisturbed vegetation. Future studies should include more detailed land use scenarios to better account for historic and future land use change in the study region, including various scenarios for changes in plantations, crop production, urbanization or pollution and their impacts on vegetation growth. This can be achieved by using large-scale products such as the harmonized land use scenarios (Hurtt et al., 2011), by considering Shared Socio-economic Pathways (Popp et al., 2017), and also by considering local-scale land use activities such as grazing, fire management or fuelwood harvesting. Some of these factors have been included into aDGVM and aDGVM2 previously, and their impacts on vegetation structure or regional-scale vegetation patterns have been investigated (Pfeiffer et al., 2019; Scheiter et al., 2015, 2019; Scheiter & Savadogo, 2016).

Despite recent developments in vegetation modelling, there is still a need to further improve our projections of future vegetation and biogeochemical cycles in order to provide reliable information for decision-making. First, we need an improved understanding of the effects of elevated CO<sub>2</sub> on vegetation, and how CO<sub>2</sub> fertilization is influenced by source or sink dynamics (Körner, 2015), microbial communities (Terrer, Vicca, Hungate, Phillips, & Prentice, 2016), nutrient limitation and temperature or drought stress. Open-top chamber experiments or FACE experiments are required in the study region to enhance our knowledge. Second, the topography of tropical Asia is complex and heterogeneous in comparison to Africa or lowland rain forests of tropical South America. Tropical Asia includes numerous islands and the Himalayas. This complexity also implies high diversity of species and biome types (Kumar & Scheiter, 2019). Improving vegetation models by including, for example, slope and aspect, and associated impacts on radiation balance, hydrology, dispersal and migration, will improve our understanding of future vegetation. Third, high-resolution climate data from process-based downscaling and accurate soil data are required to account for environmental heterogeneity. Fourth, vegetation models require a capacity to represent the various vegetation types forming biomes of tropical Asia. Vegetation types such as bamboo thickets or mangroves are typically not included in DGVMs, and aDGVM2 does not simulate giant trees present in Asian forests. Kumar and Scheiter (2019) proposed concepts on how to model these vegetation types. Finally, changes of the land surface due to simulated vegetation and phenology change or land use change modify albedo, as well as the water and carbon cycle. These changes influence the climate system via complex feedbacks (Bonan, 2008). Assessments of such feedbacks require coupling of aDGVM2 with climate models.

## 5 | CONCLUSIONS

We found that climate change and CO<sub>2</sub> fertilization will likely increase woody biomass in tropical Asia until 2099. This trend was robust for an ensemble of different climate change scenarios and different climate models. Changes in aboveground biomass were associated with changes in phenology and vegetation structure, particularly with transitions from small deciduous vegetation to tall evergreen vegetation. These findings indicate that natural vegetation in tropical Asia will remain a carbon sink until 2099 with a high potential for carbon sequestration. Any human conversion of such natural vegetation into cropland might pose a threat to the carbon sink, as croplands and plantations typically store less carbon than natural vegetation. However, the trend towards more vegetation biomass also implies a risk for ecosystems with low woody cover, such as ancient grasslands or savannas. These ecosystems were most vulnerable to climate change impacts in our simulations, and a decrease in their extent and associated losses of biodiversity is likely. Conservation of these ecosystems is therefore required. Our results indicate a high potential for carbon sequestration initiatives, and at the same time indicate a high risk of vegetation change in

ecosystems with low woody cover in protected areas. A careful balance of biodiversity conservation against carbon sequestration initiatives in the context of climate change adaptation and mitigation is mandatory.

## ACKNOWLEDGEMENTS

S.S. and D.K. thank the Deutsche Forschungsgemeinschaft (DFG) for funding (Emmy Noether grant SCHE 1719/2-1). M.P. and C.M. acknowledge funding by the German Federal Ministry of Education and Research (BMBF, SPACES2 initiative, 'SALLnet' project, grant 01LL1802B and 'EMSAfrica' project, grant 01LL1801B). R.S.L. is sponsored by CAS-TWAS President's Fellowship for International Doctoral Students (grant 2016CTF096). This research was also supported by a joint Natural Science Foundation of China–Yunnan Government grant to K.W.T. and R.T.C. (U1502264).

## CONFLICT OF INTEREST

The authors declare that they have no conflict of interest.








## AUTHOR CONTRIBUTION

S.S., K.W.T., R.T.C., R.S.L. and D.K. conceived the study; D.K. conducted model simulation runs; S.S. and D.K. analysed the data; D.K., L.L., M.P., C.M. and S.S. contributed to model development; S.S. led the writing with contributions from all co-authors.

## DATA AVAILABILITY STATEMENT

The presented data, scripts, as well as the aDGVM2 code are available upon request from the first author.

## ORCID

Simon Scheiter  <https://orcid.org/0000-0002-5449-841X>  
 Dushyant Kumar  <https://orcid.org/0000-0002-0415-3835>  
 Richard T. Corlett  <https://orcid.org/0000-0002-2508-9465>  
 Camille Gaillard  <https://orcid.org/0000-0002-5184-5279>  
 Liam Langan  <https://orcid.org/0000-0002-4765-9510>  
 Ralph Sédric Lapuz  <https://orcid.org/0000-0002-5072-2306>  
 Carola Martens  <https://orcid.org/0000-0003-3954-039X>  
 Mirjam Pfeiffer  <https://orcid.org/0000-0003-2982-3548>  
 Kyle W. Tomlinson  <https://orcid.org/0000-0003-3039-6766>

## REFERENCES

- Adole, T., Dash, J., & Atkinson, P. M. (2018). Large-scale prerain vegetation green-up across Africa. *Global Change Biology*, 24, 4054–4068. <https://doi.org/10.1111/gcb.14310>
- Blanco, C. C., Scheiter, S., Sosinski, E., Fidelis, A., Anand, M., & Pillar, V. D. (2014). Feedbacks between vegetation and disturbance processes promote long-term persistence of forest–grassland mosaics in south Brazil. *Ecological Modelling*, 291, 224–232. <https://doi.org/10.1016/j.ecolmodel.2014.07.024>
- Bonan, G. B. (2008). Forests and climate change: Forcings, feedbacks, and the climate benefits of forests. *Science*, 320, 1444–1449. <https://doi.org/10.1126/science.1155121>
- Bond, W. J. (2008). What limits trees in  $C_4$  grasslands and savannas? *Annual Review of Ecology Evolution and Systematics*, 39, 641–659. <https://doi.org/10.1146/annurev.ecolsys.39.110707.173411>
- Bond, W. J., Midgley, G. F., & Woodward, F. I. (2003). The importance of low atmospheric  $CO_2$  and fire in promoting the spread of grasslands and savannas. *Global Change Biology*, 9, 973–982. <https://doi.org/10.1046/j.1365-2486.2003.00577.x>
- Bond, W. J., Stevens, N., Midgley, G. F., & Lehmann, C. E. R. (2019). The trouble with trees: Afforestation plans for Africa. *Trends in Ecology & Evolution*, 34, 963–965. <https://doi.org/10.1016/j.tree.2019.08.003>
- Buitenwerf, R., Bond, W. J., Stevens, N., & Trollope, W. S. W. (2012). Increased tree densities in South African savannas: >50 years of data suggests  $CO_2$  as a driver. *Global Change Biology*, 18, 675–684. <https://doi.org/10.1111/j.1365-2486.2011.02561.x>
- Buitenwerf, R., Rose, L., & Higgins, S. I. (2015). Three decades of multi-dimensional change in global leaf phenology. *Nature Climate Change*, 5, 364–368. <https://doi.org/10.1038/nclimate2533>
- Chaturvedi, R. K., Gopalakrishnan, R., Jayaraman, M., Bala, G., Joshi, N. V., Sukumar, R., & Ravindranath, N. H. (2011). Impact of climate change on Indian forests: A dynamic vegetation modeling approach. *Mitigation and Adaptation Strategies for Global Change*, 16, 119–142. <https://doi.org/10.1007/s11027-010-9257-7>
- Chen, J. M., Ju, W., Ciais, P., Viovy, N., Liu, R., Liu, Y., & Lu, X. (2019). Vegetation structural change since 1981 significantly enhanced the terrestrial carbon sink. *Nature Communications*, 10, 4259. <https://doi.org/10.1038/s41467-019-12257-8>
- Cleland, E. E., Chuine, I., Menzel, A., Mooney, H. A., & Schwartz, M. D. (2007). Shifting plant phenology in response to global change. *Trends in Ecology & Evolution*, 22, 357–365. <https://doi.org/10.1016/j.tree.2007.04.003>
- Conradi, T., Slingsby, J. A., Midgley, G. F., Nottebrock, H., Schweiger, A. H., & Higgins, S. I. (2020). An operational definition of the biome for global change research. *New Phytologist*. <https://doi.org/10.1111/nph.16580>
- Corlett, R. T. (2009). Seed dispersal distances and plant migration potential in tropical East Asia. *Biotropica*, 41, 592–598. <https://doi.org/10.1111/j.1744-7429.2009.00503.x>
- Corlett, R. T., & Westcott, D. A. (2013). Will plant movements keep up with climate change? *Trends in Ecology & Evolution*, 28, 482–488. <https://doi.org/10.1016/j.tree.2013.04.003>
- Deng, Q., Zhou, G., Liu, J., Liu, S., Duan, H., & Zhang, D. (2010). Responses of soil respiration to elevated carbon dioxide and nitrogen addition in young subtropical forest ecosystems in China. *Biogeosciences*, 7, 315–328. <https://doi.org/10.5194/bg-7-315-2010>
- Ge, J., & Xie, Z. (2017). Geographical and climatic gradients of evergreen versus deciduous broad-leaved tree species in subtropical China: Implications for the definition of the mixed forest. *Ecology and Evolution*, 7, 3636–3644. <https://doi.org/10.1002/ece3.2967>
- Graham, V., Laurance, S. G., Grech, A., McGregor, A., & Venter, O. (2016). A comparative assessment of the financial costs and carbon benefits of REDD+ strategies in Southeast Asia. *Environmental Research Letters*, 11, 114022. <https://doi.org/10.1088/1748-9326/11/11/114022>
- Hannah, L., Roehrdanz, P. R., Marquet, P. A., Enquist, B. J., Midgley, G., Foden, W. ... Svenning, J.-C. (2020). 30% land conservation and climate action reduces tropical extinction risk by more than 50%. *Ecography*. <https://doi.org/10.1111/ecog.05166>
- Hantson, S., Arneth, A., Harrison, S. P., Kelley, D. I., Prentice, I. C., Rabin, S. S., ... Yue, C. (2016). The status and challenge of global fire modelling. *Biogeosciences*, 13, 3359–3375. <https://doi.org/10.5194/bg-13-3359-2016>
- Haverd, V., Smith, B., Canadell, J. G., Cuntz, M., Mikaloff-Fletcher, S., Farquhar, G., ... Trudinger, C. M. (2020). Higher than expected  $CO_2$  fertilization inferred from leaf to global observations. *Global Change Biology*, 26, 2390–2402. <https://doi.org/10.1111/gcb.14950>
- Haxeltine, A., & Prentice, I. C. (1996). Biome3: An equilibrium terrestrial biosphere model based on ecophysiological constraints, resource

- availability, and competition among plant functional types. *Global Biogeochemical Cycles*, 10, 693–709. <https://doi.org/10.1029/96GB02344>
- Hickler, T., Prentice, I. C., Smith, B., Sykes, M. T., & Zaehle, S. (2006). Implementing plant hydraulic architecture within the LPJ dynamic global vegetation model. *Global Ecology and Biogeography*, 15, 567–577. <https://doi.org/10.1111/j.1466-8238.2006.00254.x>
- Hickler, T., Rammig, A., & Werner, C. (2015). Modelling CO<sub>2</sub> impacts on forest productivity. *Current Forestry Reports*, 1(2), 69–80. <https://doi.org/10.1007/s40725-015-0014-8>
- Higgins, S. I., Buitenwerf, R., & Moncrieff, G. R. (2016). Defining functional biomes and monitoring their change globally. *Global Change Biology*, 22, 3583–3593. <https://doi.org/10.1111/gcb.13367>
- Higgins, S. I., & Scheiter, S. (2012). Atmospheric CO<sub>2</sub> forces abrupt vegetation shifts locally, but not globally. *Nature*, 488, 209–212. <https://doi.org/10.1038/nature11238>
- Hijioka, Y., Lin, E., Pereira, J. J., Corlett, R. T., Cui, X., Insarov, G. E., ... Surjan, A. (2014). Asia. In V. R. Barros, C. B. Field, D. J. Dokken, M. D. Mastrandrea, K. J. Mach, T. E. Bilir, ... L. L. White (Eds.), *Climate change 2014: Impacts, adaptation, and vulnerability. Part B: Regional aspects. Contribution of working group II to the fifth assessment report of the Intergovernmental Panel on Climate Change* (pp. 1327–1370). Cambridge, UK and New York, NY: Cambridge University Press.
- Hijmans, R. J. (2020). *raster: Geographic data analysis and modeling*. R package version 3.0-12. Retrieved from <https://CRAN.R-project.org/package=raster>
- Hiremath, A. J., & Sundaram, B. (2005). The fire-lantana cycle hypothesis in Indian forests. *Conservation and Society*, 3, 26–42.
- Hubau, W., Lewis, S. L., Phillips, O. L., Affum-Baffoe, K., Beeckman, H., Cuní-Sánchez, A., ... Zemagho, L. (2020). Asynchronous carbon sink saturation in African and Amazonian tropical forests. *Nature*, 579, 80–87. <https://doi.org/10.1038/s41586-020-2035-0>
- Hughes, A. C. (2017). Understanding the drivers of Southeast Asian biodiversity loss. *Ecosphere*, 8, e01624. <https://doi.org/10.1002/ecs2.1624>
- Hurt, G. C., Chini, L. P., Frolking, S., Betts, R. A., Feddema, J., Fischer, G., ... Jones, C. D. (2011). Harmonization of land-use scenarios for the period 1500–2100: 600 years of global gridded annual land-use transitions, wood harvest, and resulting secondary lands. *Climatic Change*, 109, 117–161. <https://doi.org/10.1007/s10584-011-0153-2>
- IPCC. (2018). Global warming of 1.5°C. An IPCC Special Report on the impacts of global warming of 1.5°C above pre-industrial levels and related global greenhouse gas emission pathways, in the context of strengthening the global response to the threat of climate change, sustainable development, and efforts to eradicate poverty, chap. In V. Masson-Delmotte, P. Zhai, H. O. Poertner, D. Roberts, J. Skea, P. R. Shukla, A. Pirani, W. Moufouma-Okia, C. Pean, R. Pidcock, S. Connors, J. B. R. Matthews, Y. Chen, X. Zhou, M. I. Gomis, E. Lonnoy, T. Maycock, M. Tignor, & T. Waterfield (Eds.), *Summary for policymakers* (pp. 1–24). Geneva, Switzerland: World Meteorological Organization.
- Jarvis, A., Reuter, H. I., Nelson, A., & Guevara, E. (2008). *Hole-filled srtm for the globe version 4*. Retrieved from the [cgiar-csi srtm 90m database](http://srtm.csi.cgiar.org) <http://srtm.csi.cgiar.org>
- Kannan, R., Shackleton, C. M., & Uma Shaanker, R. (2013). Reconstructing the history of introduction and spread of the invasive species, lantana, at three spatial scales in India. *Biological Invasions*, 15, 1287–1302. <https://doi.org/10.1007/s10530-012-0365-z>
- Kgope, B. S., Bond, W. J., & Midgley, G. F. (2010). Growth responses of African savanna trees implicate atmospheric [CO<sub>2</sub>] as a driver of past and current changes in savanna tree cover. *Austral Ecology*, 35, 451–463. <https://doi.org/10.1111/j.1442-9993.2009.02046.x>
- Körner, C. (2015). Paradigm shift in plant growth control. *Current Opinion in Plant Biology*, 25, 107–114. <https://doi.org/10.1016/j.pbi.2015.05.003>
- Kumar, D., Pfeiffer, M., Gaillard, C., Langan, L., Martens, C., & Scheiter, S. (2020). Misinterpretation of Asian savannas as degraded forest can mislead management and conservation policy under climate change. *Biological Conservation*, 241, 108293. <https://doi.org/10.1016/j.biocon.2019.108293>
- Kumar, D., Pfeiffer, M., Gaillard, C., Langan, L., & Scheiter, S. (2020). Climate change and elevated CO<sub>2</sub> favor forest over savanna under different future scenarios in South Asia. *Biogeosciences Discussions*, 2020, 1–34.
- Kumar, D., & Scheiter, S. (2019). Biome diversity in South Asia – How can we improve vegetation models to understand global change impact at regional level? *Science of the Total Environment*, 671, 1001–1016. <https://doi.org/10.1016/j.scitotenv.2019.03.251>
- Langan, L. (2019). *Holism in plant biogeography – Improving the representation of, and interactions between the biosphere, hydrosphere, atmosphere and pedosphere*. PhD thesis, Institute of Physical Geography, Goethe University Frankfurt am Main, Germany.
- Langan, L., Higgins, S. I., & Scheiter, S. (2017). Climate-biomes, pedo-biomes or pyro-biomes: Which world view explains the tropical forest – Savanna boundary in South America? *Journal of Biogeography*, 44, 2319–2330. <https://doi.org/10.1111/jbi.13018>
- Le Quéré, C., Andrew, R. M., Friedlingstein, P., Sitch, S., Hauck, J., Pongratz, J., ... Zheng, B. O. (2018). Global carbon budget 2018. *Earth System Science Data*, 10, 2141–2194. <https://doi.org/10.5194/essd-10-2141-2018>
- Liu, J. X., Zhang, D. Q., Zhou, G. Y., Faivre-Vuillin, B., Deng, Q., & Wang, C. L. (2008). CO<sub>2</sub> enrichment increases nutrient leaching from model forest ecosystems in subtropical China. *Biogeosciences*, 5, 1783–1795. <https://doi.org/10.5194/bg-5-1783-2008>
- Liu, Y., Piao, S., Gasser, T., Ciais, P., Yang, H., Wang, H., ... Wang, K. (2019). Field-experiment constraints on the enhancement of the terrestrial carbon sink by CO<sub>2</sub> fertilization. *Nature Geoscience*, 12, 809–814. <https://doi.org/10.1038/s41561-019-0436-1>
- Loarie, S. R., Duffy, P. B., Hamilton, H., Asner, G. P., Field, C. B., & Ackerly, D. D. (2009). The velocity of climate change. *Nature*, 462, 1052–1055. <https://doi.org/10.1038/nature08649>
- Martens, C., Hickler, T., Davis-Reddy, C., Engelbrecht, F., Higgins, S. I., von Maltitz, G. P., ... Scheiter, S. (under review). Large uncertainties in future biome changes in Africa call for flexible climate adaptation strategies.
- Midgley, G. F., & Bond, W. J. (2015). Future of African terrestrial biodiversity and ecosystems under anthropogenic climate change. *Nature Climate Change*, 5, 823–829. <https://doi.org/10.1038/nclimate2753>
- Moncrieff, G. R., Bond, W. J., & Higgins, S. I. (2016). Revising the biome concept for understanding and predicting global change impacts. *Journal of Biogeography*, 43, 863–873. <https://doi.org/10.1111/jbi.12701>
- Moncrieff, G. R., Scheiter, S., Langan, L., Trabucco, A., & Higgins, S. I. (2016). The future distribution of the savannah biome: Model-based and biogeographic contingency. *Philosophical Transactions of the Royal Society B: Biological Sciences*, 371. <https://doi.org/10.1098/rstb.2015.0311>
- Mucina, L. (2019). Biome: Evolution of a crucial ecological and biogeographical concept. *New Phytologist*, 222, 97–114. <https://doi.org/10.1111/nph.15609>
- Nabel, J. E. M. S., Zurbruggen, N., & Lischke, H. (2013). Interannual climate variability and population density thresholds can have a substantial impact on simulated tree species' migration. *Ecological Modelling*, 257, 88–100. <https://doi.org/10.1016/j.ecolmodel.2013.02.015>
- Nachtergaele, F., van Velthuisen, H., & Verelst, L. (2009). *Harmonized world soil database (version 1.1)*. Rome, Italy and Laxenburg, Austria: FAO and IIASA.
- Oo, W. P., & Koike, F. (2015). Dry forest community types and their predicted distribution based on a habitat model for the central dry zone



- of Myanmar. *Forest Ecology and Management*, 358, 108–121. <https://doi.org/10.1016/j.foreco.2015.09.006>
- Ozanne, C. M. P., Anhuf, D., Boulter, S. L., Keller, M., Kitching, R. L., Körner, C., ... Stork, N. E. (2003). Biodiversity meets the atmosphere: A global view of forest canopies. *Science*, 301, 183–186. <https://doi.org/10.1126/science.1084507>
- Pachzelt, A., Rammig, A., Higgins, S. I., & Hickler, T. (2013). Coupling a physiological grazer population model with a generalized model for vegetation dynamics. *Ecological Modelling*, 263, 92–102. <https://doi.org/10.1016/j.ecolmodel.2013.04.025>
- Pfeiffer, M., Langan, L., Linstädter, A., Martens, C., Gaillard, C., Ruppert, J. C., ... Scheiter, S. (2019). Grazing and aridity reduce perennial grass abundance in semi-arid rangelands – Insights from a trait-based dynamic vegetation model. *Ecological Modelling*, 395, 11–22. <https://doi.org/10.1016/j.ecolmodel.2018.12.013>
- Piao, S., Liu, Q., Chen, A., Janssens, I. A., Fu, Y., Dai, J., ... Zhu, X. (2019). Plant phenology and global climate change: Current progresses and challenges. *Global Change Biology*, 25, 1922–1940. <https://doi.org/10.1111/gcb.14619>
- Piao, S., Wang, X., Park, T., Chen, C., Lian, X. U., He, Y., ... Myneni, R. B. (2020). Characteristics, drivers and feedbacks of global greening. *Nature Reviews Earth & Environment*, 1, 14–27. <https://doi.org/10.1038/s43017-019-0001-x>
- Piao, S., Yin, G., Tan, J., Cheng, L., Huang, M., Li, Y., ... Poulter, B. (2015). Detection and attribution of vegetation greening trend in China over the last 30 years. *Global Change Biology*, 21, 1601–1609. <https://doi.org/10.1111/gcb.12795>
- Popp, A., Calvin, K., Fujimori, S., Havlik, P., Humpenöder, F., Stehfest, E., ... Vuuren, D. P. V. (2017). Land-use futures in the shared socio-economic pathways. *Global Environmental Change*, 42, 331–345. <https://doi.org/10.1016/j.gloenvcha.2016.10.002>
- Prentice, I., Bondeau, A., Cramer, W., Harrison, S. P., Hickler, T., Lucht, W., ... Sykes, M. T. (2007). Dynamic global vegetation modeling: Quantifying terrestrial ecosystem responses to large-scale environmental change. In J. G. Canadell D. E. Pataki & L. F. Pitelka (Eds.), *Terrestrial ecosystems in a changing world*, (pp. 175–192). Berlin, Heidelberg: Springer.
- R Core Team. (2018). *R: A language and environment for statistical computing*. Vienna, Austria: R Foundation for Statistical Computing. <https://www.R-project.org/>
- Raghavan, S. V., Liu, J., Nguyen, N. S., Vu, M. T., & Liong, S. Y. (2018). Assessment of CMIP5 historical simulations of rainfall over Southeast Asia. *Theoretical and Applied Climatology*, 132, 989–1002. <https://doi.org/10.1007/s00704-017-2111-z>
- Ralhan, P. K., Khanna, R. K., Singh, S. P., & Singh, J. S. (1985). Phenological characteristics of the tree layer of Kumaun Himalayan forests. *Vegetatio*, 60, 91–101. <https://doi.org/10.1007/BF00040351>
- Ratnam, J., Bond, W. J., Fensham, R. J., Hoffmann, W. A., Archibald, S., Lehmann, C. E. R., ... Sankaran, M. (2011). When is a ‘forest’ a savanna, and why does it matter? *Global Ecology and Biogeography*, 20, 653–660. <https://doi.org/10.1111/j.1466-8238.2010.00634.x>
- Ratnam, J., Tomlinson, K. W., Rasquinha, D. N., & Sankaran, M. (2016). Savannas of Asia: Antiquity, biogeography, and an uncertain future. *Philosophical Transactions of the Royal Society B: Biological Sciences*, 371, 20150305. <https://doi.org/10.1098/rstb.2015.0305>
- Ravindranath, N. H., Joshi, N. V., Sukumar, R., & Saxena, A. (2006). Impact of climate change on forests in India. *Current Science*, 90, 354–361.
- Reick, C. H., Raddatz, T., Brovkin, V., & Gayler, V. (2013). Representation of natural and anthropogenic land cover change in MPI-ESM. *Journal of Advances in Modeling Earth Systems*, 5, 459–482. <https://doi.org/10.1002/jame.20022>
- Saatchi, S. S., Harris, N. L., Brown, S., Lefsky, M., Mitchard, E. T. A., Salas, W., ... Morel, A. (2011). Benchmark map of forest carbon stocks in tropical regions across three continents. *Proceedings of the National Academy of Sciences of the United States of America*, 108, 9899–9904. <https://doi.org/10.1073/pnas.1019576108>
- Sankaran, M., Hanan, N. P., Scholes, R. J., Ratnam, J., Augustine, D. J., Cade, B. S., ... Zambatis, N. (2005). Determinants of woody cover in African savannas. *Nature*, 438, 846–849. <https://doi.org/10.1038/nature04070>
- Sato, H., & Ise, T. (2012). Effect of plant dynamic processes on African vegetation responses to climate change: Analysis using the spatially explicit individual-based dynamic global vegetation model (SEIB-DGVM). *Journal of Geophysical Research: Biogeosciences*, 117, G03017. <https://doi.org/10.1029/2012JG002056>
- Sato, H., Itoh, A., & Kohyama, T. (2007). SEIB-DGVM: A new dynamic global vegetation model using a spatially explicit individual-based approach. *Ecological Modelling*, 200, 279–307. <https://doi.org/10.1016/j.ecolmodel.2006.09.006>
- Scheiter, S., & Higgins, S. I. (2009). Impacts of climate change on the vegetation of Africa: An adaptive dynamic vegetation modelling approach (aDGVM). *Global Change Biology*, 15, 2224–2246. <https://doi.org/10.1111/j.1365-2486.2008.01838.x>
- Scheiter, S., Higgins, S. I., Beringer, J., & Hutley, L. B. (2015). Climate change and long-term fire management impacts on Australian savannas. *New Phytologist*, 205, 1211–1226. <https://doi.org/10.1111/nph.13130>
- Scheiter, S., Langan, L., & Higgins, S. I. (2013). Next generation dynamic global vegetation models: Learning from community ecology. *New Phytologist*, 198, 957–969. <https://doi.org/10.1111/nph.12210>
- Scheiter, S., Moncrieff, G. R., Pfeiffer, M., & Higgins, S. I. (2020). African biomes are most sensitive to changes in CO<sub>2</sub> under recent and near-future CO<sub>2</sub> conditions. *Biogeosciences*, 17, 1147–1167. <https://doi.org/10.5194/bg-17-1147-2020>
- Scheiter, S., & Savadogo, P. (2016). Ecosystem management can mitigate vegetation shifts induced by climate change in West Africa. *Ecological Modelling*, 332, 19–27. <https://doi.org/10.1016/j.ecolmodel.2016.03.022>
- Scheiter, S., Schulte, J., Pfeiffer, M., Martens, C., Erasmus, B. F. N., & Twine, W. C. (2019). How does climate change influence the economic value of ecosystem services in savanna rangelands? *Ecological Economics*, 157, 342–356. <https://doi.org/10.1016/j.jecolecon.2018.11.015>
- Schleuning, M., Fründ, J., Schweiger, O., Welk, E., Albrecht, J., Albrecht, M., ... Hof, C. (2016). Ecological networks are more sensitive to plant than to animal extinction under climate change. *Nature Communications*, 7, 13965. <https://doi.org/10.1038/ncomms13965>
- Simard, M., Pinto, N., Fisher, J. B., & Baccini, A. (2011). Mapping forest canopy height globally with spaceborne lidar. *Journal of Geophysical Research: Biogeosciences*, 116, G04021. <https://doi.org/10.1029/2011JG001708>
- Sitch, S., Huntingford, C., Gedney, N., Levy, P. E., Lomas, M., Piao, S. L., ... Woodward, F. I. (2008). Evaluation of the terrestrial carbon cycle, future plant geography and climate-carbon cycle feedbacks using five Dynamic Global Vegetation Models (DGVMs). *Global Change Biology*, 14, 2015–2039. <https://doi.org/10.1111/j.1365-2486.2008.01626.x>
- Smit, I. P. J., & Prins, H. H. T. (2015). Predicting the effects of woody encroachment on mammal communities, grazing biomass and fire frequency in African savannas. *PLoS One*, 10, e0137857. <https://doi.org/10.1371/journal.pone.0137857>
- Smith, B., Wärlind, D., Arneth, A., Hickler, T., Leadley, P., Siltberg, J., & Zaehle, S. (2014). Implications of incorporating N cycling and N limitations on primary production in an individual-based dynamic vegetation model. *Biogeosciences*, 11, 2027–2054. <https://doi.org/10.5194/bg-11-2027-2014>
- Soh, W. K., Yiotis, C., Murray, M., Parnell, A., Wright, I. J., Spicer, R. A., ... McElwain, J. C. (2019). Rising CO<sub>2</sub> drives divergence in water use efficiency of evergreen and deciduous plants. *Science Advances*, 5, eaax7906. <https://doi.org/10.1126/sciadv.aax7906>
- Stevens, N., Lehmann, C. E. R., Murphy, B. P., & Durigan, G. (2017). Savanna woody encroachment is widespread across three continents. *Global Change Biology*, 23, 235–244. <https://doi.org/10.1111/gcb.13409>



- Still, C. J., Berry, J. A., Collatz, G. J., & DeFries, R. S. (2003). Global distribution of  $C_3$  and  $C_4$  vegetation: Carbon cycle implications. *Global Biogeochemical Cycles*, 17, 1006. <https://doi.org/10.1029/2001gb001807>
- Symes, W. S., Rao, M., Mascia, M. B., & Carrasco, L. R. (2016). Why do we lose protected areas? Factors influencing protected area downgrading, downsizing and degazettement in the tropics and subtropics. *Global Change Biology*, 22, 656–665. <https://doi.org/10.1111/gcb.13089>
- Terrer, C., Vicca, S., Hungate, B. A., Phillips, R. P., & Prentice, I. C. (2016). Mycorrhizal association as a primary control of the  $CO_2$  fertilization effect. *Science*, 353, 72–74. <https://doi.org/10.1126/science.aaf4610>
- Tews, J., Brose, U., Grimm, V., Tielbörger, K., Wichmann, M. C., Schwager, M., & Jeltsch, F. (2004). Animal species diversity driven by habitat heterogeneity/diversity: The importance of keystone structures. *Journal of Biogeography*, 31, 79–92. <https://doi.org/10.1046/j.0305-0270.2003.00994.x>
- Thuiller, W., Lavorel, S., Araujo, M. B., Sykes, M. T., & Prentice, I. C. (2005). Climate change threats to plant diversity in Europe. *Proceedings of the National Academy of Sciences of the United States of America*, 102, 8245–8250. <https://doi.org/10.1073/pnas.0409902102>
- Tuanmu, M. N., & Jetz, W. (2014). A global 1-km consensus land-cover product for biodiversity and ecosystem modelling. *Global Ecology and Biogeography*, 23, 1031–1045. <https://doi.org/10.1111/geb.12182>
- van Vuuren, D. P., Edmonds, J., Kainuma, M., Riahi, K., Thomson, A., Hibbard, K., ... Rose, S. K. (2011). The representative concentration pathways: An overview. *Climatic Change*, 109, 5–31. <https://doi.org/10.1007/s10584-011-0148-z>
- Verheijen, L. M., Brovkin, V., Aerts, R., Bönisch, G., Cornelissen, J. H. C., Kattge, J., ... van Bodegom, P. M. (2013). Impacts of trait variation through observed trait-climate relationships on performance of an Earth system model: A conceptual analysis. *Biogeosciences*, 10, 5497–5515. <https://doi.org/10.5194/bg-10-5497-2013>
- Walther, G. R. (2010). Community and ecosystem responses to recent climate change. *Philosophical Transactions of the Royal Society B: Biological Sciences*, 365, 2019–2024. <https://doi.org/10.1098/rstb.2010.0021>
- Warszawski, L., Frieler, K., Huber, V., Piontek, F., Serdeczny, O., & Schewe, J. (2014). The Inter-Sectoral Impact Model Intercomparison Project (ISI-MIP): Project framework. *Proceedings of the National Academy of Sciences of the United States of America*, 111, 3228–3232. <https://doi.org/10.1073/pnas.1312330110>
- Yu, M., Wang, G., Parr, D., & Ahmed, K. F. (2014). Future changes of the terrestrial ecosystem based on a dynamic vegetation model driven with RCP8.5 climate projections from 19 GCMs. *Climatic Change*, 127, 257–271. <https://doi.org/10.1007/s10584-014-1249-2>
- Zachos, F. E., & Habel, J. C. (Eds.). (2011). *Biodiversity hotspots. Distribution and protection of conservation priority areas*. Berlin and Heidelberg, Germany: Springer-Verlag.
- Zeng, Z., Piao, S., Li, L. Z. X., Zhou, L., Ciais, P., Wang, T., ... Wang, Y. (2017). Climate mitigation from vegetation biophysical feedbacks during the past three decades. *Nature Climate Change*, 7, 432–436. <https://doi.org/10.1038/nclimate3299>
- Zhang, Y., Zhu, Z., Liu, Z., Zeng, Z., Ciais, P., Huang, M., ... Piao, S. (2016). Seasonal and interannual changes in vegetation activity of tropical forests in Southeast Asia. *Agricultural and Forest Meteorology*, 224, 1–10. <https://doi.org/10.1016/j.agrformet.2016.04.009>

## SUPPORTING INFORMATION

Additional supporting information may be found online in the Supporting Information section.

**How to cite this article:** Scheiter S, Kumar D, Corlett RT, et al. Climate change promotes transitions to tall evergreen vegetation in tropical Asia. *Glob Change Biol*. 2020;26:5106–5124. <https://doi.org/10.1111/gcb.15217>